Journal of
Materials Chemistry A

ROYAL SOCIETY
OF CHEMISTRY

REVIEW

View Article Online
View Journal

Check for updates

Cite this: DOI: 10.1039/d6ta00813e

Monometallic nickel as a tunable electrocatalyst for alkaline hydrogen evolution: a critical review

Ioannis Poimenidis * and Michalis Konsolakis*

The hydrogen evolution reaction (HER) is a cornerstone of water electrolysis technologies for sustainable hydrogen production. Nickel-based catalysts have emerged as leading non-precious alternatives to platinum due to their abundance, electrochemical stability in alkaline environments, and tunable physicochemical properties. This review critically examines recent advances in the synthesis, surface/interface modification, and performance optimization of monometallic Ni HER electrodes, emphasizing how rational engineering can elevate their reactivity toward state-of-the-art levels. A comprehensive overview of fabrication techniques, including electrodeposition, hydrothermal synthesis, pulsed laser deposition (PLD), physical vapor deposition (PVD), laser nanomachining, and chemical vapor deposition (CVD), is presented with a focus on how these methods tailor microstructure, active-site density, and interfacial chemistry. Special attention is given to engineering strategies such as defect induction (*e.g.*, oxygen vacancies), interface engineering, and hierarchical nanostructuring, which regulate surface reactivity, charge-transfer behavior, and catalytic efficiency. Across the literature, these approaches have produced monometallic Ni electrodes with overpotentials as low as ~40–50 mV at 10 mA cm^{-2}, and Tafel slopes in the range of 55–65 mV dec^{-1}, values that approach or, in some cases, rival those of multicomponent Ni-based electrocatalysts (*e.g.*, Ni–Mo, Ni–Fe) and significantly narrow the performance gap to Pt-group materials under alkaline conditions. By systematically correlating synthesis routes, structural descriptors, and HER metrics, this review demonstrates how monometallic Ni can achieve high intrinsic activity, robust durability, and industrially relevant current densities without relying on noble metals or complex alloying. Furthermore, by outlining a strategic roadmap to translate these lab-scale advances into scalable manufacturing processes, these insights establish monometallic nickel not only as a benchmark model system for mechanistic studies but also as a technologically viable catalyst platform for next-generation alkaline hydrogen production.

Received 27th January 2026
Accepted 23rd March 2026

DOI: 10.1039/d6ta00813e

rsc.li/materials-a

Lab of Materials Science and Processes, School of Production Engineering & Management, Technical University of Crete, 73100 Chania, Crete, Greece. E-mail: ipoimenidis@tuc.gr; mkonsolakis@tuc.gr

Ioannis Poimenidis

Dr Ioannis Poimenidis is a researcher at the Technical University of Crete, Greece, specializing in electrochemistry and materials science, with expertise in nanostructured electrode design and energy-related applications. His work focuses on electrocatalysis, particularly the hydrogen evolution reaction (HER) and oxygen evolution reaction (OER), as well as advanced electrode architectures for supercapacitors and water electrolysis systems. His research emphasizes defect engineering, surface and interface engineering, and the development of materials with enhanced electrochemical performance.

Michalis Konsolakis

Dr Michalis Konsolakis is a Professor at the Technical University of Crete, Greece and Director of Materials Science and Processes Lab. His research primarily focuses on heterogeneous catalysis, electrocatalysis, and surface science, with a particular emphasis on structure–property relationships. His current work investigates the rational design and nano-engineering of electro-catalytic materials using advanced synthetic and promotional methodologies.

1. Introduction

The escalating global energy demand, the imminent fossil fuels crisis, and calls for a transition to green energy have led the political and research communities to pursue alternative, environmentally friendly energy such as wind, solar, and hydrogen.[1,2] To effectively harness the potential of sustainable energy resources, the development of efficient energy conversion technologies is of paramount importance.[3] While all environmentally friendly energy sources play a crucial role in addressing the planet's urgent pollution problem, most are adversely affected by temporal and weather variability, resulting in low energy delivery efficiency.[4,5] On the other hand, hydrogen energy production is much more flexible than the aforementioned energy sources. In addition, hydrogen provides an excellent energy density (142 MJ kg^{-1}, upper heating value), is considered the ultimate clean energy carrier, and produces only water as a byproduct during combustion.[6]

Electrochemical water splitting is a process where hydrogen gas is generated at the cathode and oxygen gas at the anode. These occur through the hydrogen evolution reaction (HER) and oxygen evolution reaction (OER), respectively. To drive these reactions, an external electric current is applied to overcome the energy barrier, which is approximately 237 kJ mol^{-1}. Efficient water electrolysis requires the development of catalysts that can accelerate the electrochemical reactions occurring at both electrodes, including the hydrogen evolution reaction (HER) at the cathode, which governs the rate of hydrogen generation.[2] This kinetic limitation increases the overpotential, which, in turn, raises the overall energy consumption and the cost of the electrolysis system.[7]

In the HER, protons in acidic media ($2H^+ + 2e^- \leftrightarrow H_2$) or water molecules in alkaline media ($2H_2O + 2e^- \leftrightarrow H_2 + 2OH^-$) are reduced to produce hydrogen gas.[8] Due to the inherently slow reaction rates, efficient electrocatalysts are essential to lower the activation energy and accelerate the process.[9] Reducing the cathodic overpotential is therefore a key strategy to improve the overall efficiency and cost-effectiveness of electrochemical water splitting. Numerous materials acting as catalysts are reported in the literature that could meet the appropriate criteria for a suitable electrode for HER, such as high catalytic activity, chemical and mechanical stability, and, finally, low cost.[9] An ideal HER electrode should enable efficient hydrogen production at high current densities with minimal overpotential, maintain stable operating potentials over extended operation, exhibit high chemical and electrochemical durability, adhere robustly to the substrate, resist poisoning by impurities, tolerate power fluctuations or interruptions, and be safe, environmentally benign, and cost-effective to manufacture. Consequently, the development of a truly ideal HER electrode remains a significant challenge.

Noble metals, particularly platinum (Pt), are renowned for their superior catalytic activity toward the hydrogen evolution reaction (HER), exhibiting low overpotentials and favorable Tafel slopes.[2] This exceptional performance is attributed to platinum's near-optimal hydrogen binding energy, which facilitates both the adsorption of hydrogen intermediates and their efficient desorption to form molecular hydrogen (H_2).[3] Nevertheless, the high cost and limited availability of noble metals pose substantial challenges to their large-scale deployment, particularly in hydrogen production technologies. The constrained global reserves of platinum-group metals, combined with the energy-intensive nature of their extraction, result in elevated market prices, thereby limiting their economic viability for widespread use in water electrolysis systems. Significant research efforts have focused on developing earth-abundant, cost-effective alternatives to noble-metal-based HER catalysts to address these limitations. In addition to transition metals like nickel and cobalt, several non-metal-based materials have emerged as promising candidates for HER catalysis, including heteroatom-doped carbon nanostructures (*e.g.*, N-, P-, S-doped graphene), boron-based catalysts, and graphitic carbon nitride (g-C_3N_4), owing to their tunable electronic structures, high surface areas, and intrinsic catalytic activity.[10–13] Among these, nickel (Ni) has emerged as an up-and-coming candidate due to its natural abundance, low cost, excellent electrical conductivity, intrinsic corrosion resistance in alkaline environments, and commendable electrocatalytic activity for HER.[3,14] Collectively, these properties render nickel an attractive and practical alternative to noble metals for HER electrocatalysts, particularly under alkaline conditions.

Nickel has been extensively investigated as a hydrogen evolution reaction (HER) electrocatalyst for several decades, with early studies highlighting its intrinsic catalytic activity, particularly in alkaline media.[3] Over time, advances in nanotechnology and materials science have markedly expanded the strategies available for optimizing nickel-based catalysts. Specifically, the development of diverse nanostructured architectures, including nanoparticles,[15,16] nanowires,[17–20] and porous foams[15,21–24] has resulted in a significant enhancement of catalytic performance by increasing the electrochemically active surface area and the density of accessible active sites. Consequently, the research landscape has evolved from initial investigations into the fundamental properties of bulk nickel to the deliberate and sophisticated engineering of its nanostructure to maximize catalytic efficacy.

Despite these advances, the HER performance of monometallic nickel remains inferior to that of platinum, particularly when considering the overpotential required to achieve high current densities relevant for industrial hydrogen production.[25] This performance gap underscores a critical challenge in the field and necessitates focused efforts to enhance both the intrinsic activity and the long-term operational stability of nickel-based electrodes.[26] Accordingly, various strategies have been developed, including surface functionalization, precise morphological control, heteroatom doping, and atomic-level defect engineering, all aimed at promoting more favorable reaction kinetics and improving catalyst durability. These strategies have led to the development of Ni electrocatalysts with advanced physicochemical properties and high HER electrocatalytic efficiency; however, most of them are characterized by complex/multimetallic compositions and complicated synthesis and promotion processes.[27–31]

Unlike broader reviews that emphasize multimetallic composites or alloyed Ni-based systems, the present review focuses exclusively on monometallic nickel electrodes, thereby enabling a more precise examination of their intrinsic catalytic behavior, free of dopant or synergistic alloy effects. This focused approach enables a clearer understanding of fundamental structure–activity relationships by bridging atomic-scale descriptors, such as hydrogen adsorption energy and surface coordination, with macroscopic HER performance metrics, including overpotential, Tafel slope, and durability. By systematically analyzing the influence of various synthesis techniques, surface modification strategies, and morphological architectures on nickel's HER performance, this review elucidates key mechanistic bottlenecks. Moreover, from a practical perspective, it is imperative to develop monometallic composites with the desired electrochemical performance while avoiding complex synthetic methods and compositions. Ultimately, this review aims to provide a rational design framework for advancing bare monometallic Ni HER electrodes, emphasizing their cost-effectiveness, stability in alkaline conditions, and industrial relevance, without the added complexity of multi-elemental systems.

The present review is organized into a series of interrelated sections that collectively provide a comprehensive overview of recent advances in monometallic nickel electrocatalysts for the hydrogen evolution reaction (HER). Sections 2 and 3 introduce the fundamental aspects of HER, including the reaction mechanisms on Ni surfaces and the key electrochemical parameters used to evaluate catalytic activity, kinetics, and stability. Section 4 focuses on advanced experimental and theoretical insights, highlighting the role of *in situ* and *operando* characterization techniques, in conjunction with density functional theory (DFT) calculations, in identifying the catalytically active states of Ni under HER conditions. Section 5 constitutes the core of this review and systematically discusses fine-tuning engineering strategies, namely, surface modification, interface engineering, morphology control, and defect engineering, along with their synergistic effects on hydrogen adsorption energetics, charge-transfer kinetics, and overall HER performance. Section 6 provides a critical overview of the major synthesis routes employed for fabricating monometallic Ni electrodes, correlating fabrication methods with structural characteristics and electrochemical performance metrics. Section 7 addresses the remaining challenges, scalability considerations, and future research directions for monometallic Ni-based HER electrocatalysts. Overall, this structured framework bridges fundamental mechanistic understanding with materials engineering strategies and practical considerations, offering a unified perspective on the rational design of high-performance, scalable monometallic Ni electrodes for alkaline hydrogen production. To the best of our knowledge, this represents the first systematic review dedicated exclusively to the synthesis, structural fine-tuning, and intrinsic optimization of monometallic nickel electrodes for the HER.

2. Fundamental mechanisms of the HER on nickel surfaces

The hydrogen evolution reaction (HER) on nickel substrates, as with other electrocatalytic materials, involves a sequence of elementary steps. The exact reaction pathway and the rate-determining step can vary depending on the pH of the electrolyte (acidic or alkaline) and the surface characteristics of the nickel catalyst.[8] In general, HER progresses through three key steps: the Volmer step (electrochemical adsorption), the Tafel step (chemical desorption), and the Heyrovsky step (electrochemical desorption).[8] The overall mechanism can proceed *via* two primary routes: the Volmer–Tafel mechanism or the Volmer–Heyrovsky mechanism[32] (Fig. 1).

In acidic environments, hydronium ions (H_3O^+) serve as the primary proton source. The initial Volmer step involves the electrochemical adsorption of a proton onto the nickel surface (M), with simultaneous electron transfer, forming an adsorbed hydrogen intermediate (M–H*) by the following reaction:[32]

$$H^+ + M + e^- \rightarrow M\text{–}H^* \tag{1}$$

Subsequent formation of molecular hydrogen proceeds *via* either of the following steps:

Tafel step – two adsorbed hydrogen atoms combine chemically on the surface to produce hydrogen gas:[33]

$$M\text{–}H^* + M\text{–}H^* \rightarrow H_2 + 2M \tag{2}$$

Heyrovsky step – an adsorbed hydrogen atom reacts with a proton from the solution and an electron, forming hydrogen gas *via* electrochemical desorption:[34]

$$M\text{–}H^* + H^+ + e^- \rightarrow H_2 + M \tag{3}$$

In alkaline conditions, the low concentration of free protons shifts the hydrogen source to water molecules (Fig. 1). The Volmer step now involves the electrochemical reduction of water, producing an adsorbed hydrogen atom and a hydroxide ion:[35]

Volmer step (alkaline):

$$H_2O + M + e^- \rightarrow M\text{–}H^* + OH^- \tag{4}$$

As in acidic media, molecular hydrogen can form *via* either:[35]

Tafel step:

$$M\text{–}H^* + M\text{–}H^* \rightarrow H_2 + 2M \tag{5}$$

Heyrovsky step (alkaline):

$$M\text{–}H^* + H_2O + e^- \rightarrow H_2 + M + OH^- \tag{6}$$

The dominant HER pathway on nickel depends on factors such as the hydrogen surface coverage and the strength of the nickel–hydrogen bond, often quantified by the hydrogen adsorption free energy.[36] The Tafel slope, a key experimental parameter, is widely used to infer the rate-limiting step in

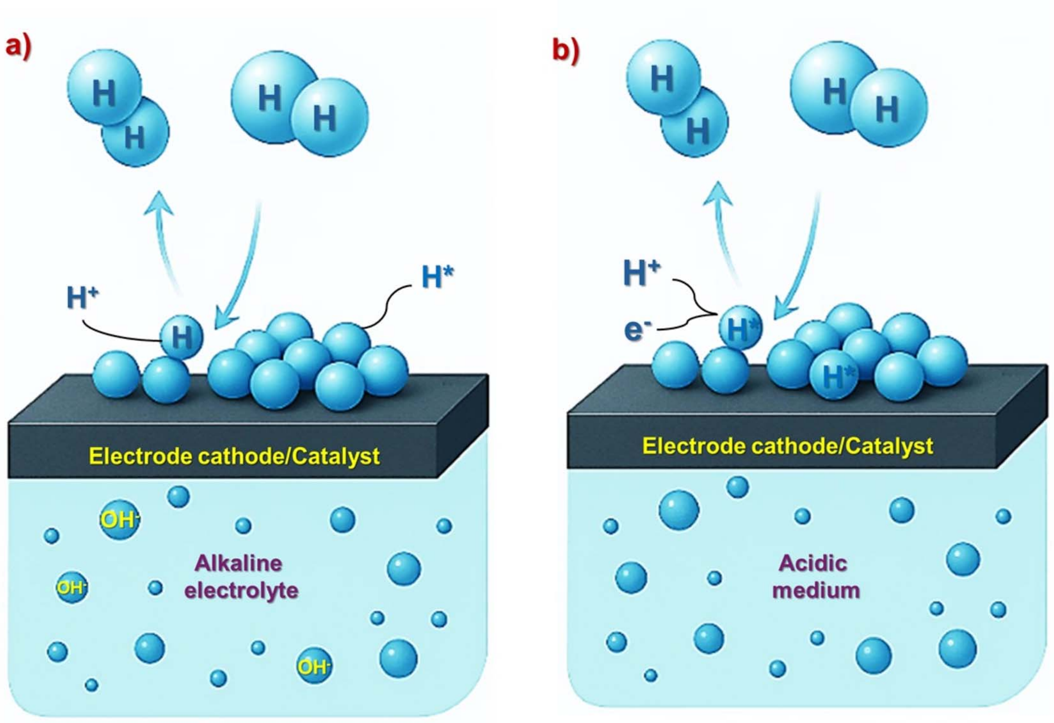

Fig. 1 Schematic illustration of the HER mechanism in alkaline medium (a) and acidic medium (b).

electrochemical reactions. A Tafel slope of ~30 mV dec^{-1} in acidic media typically indicates that the Tafel step is rate-determining. A slope of ~120 mV dec^{-1}, commonly observed under alkaline conditions, suggests that the Volmer step is rate-limiting (Fig. 2). Indeed, many studies on polycrystalline nickel in alkaline solutions report Tafel slopes of around 120 mV dec^{-1}, indicating a Volmer–Heyrovsky mechanism with the Volmer step as the rate-determining step.[37] However, these

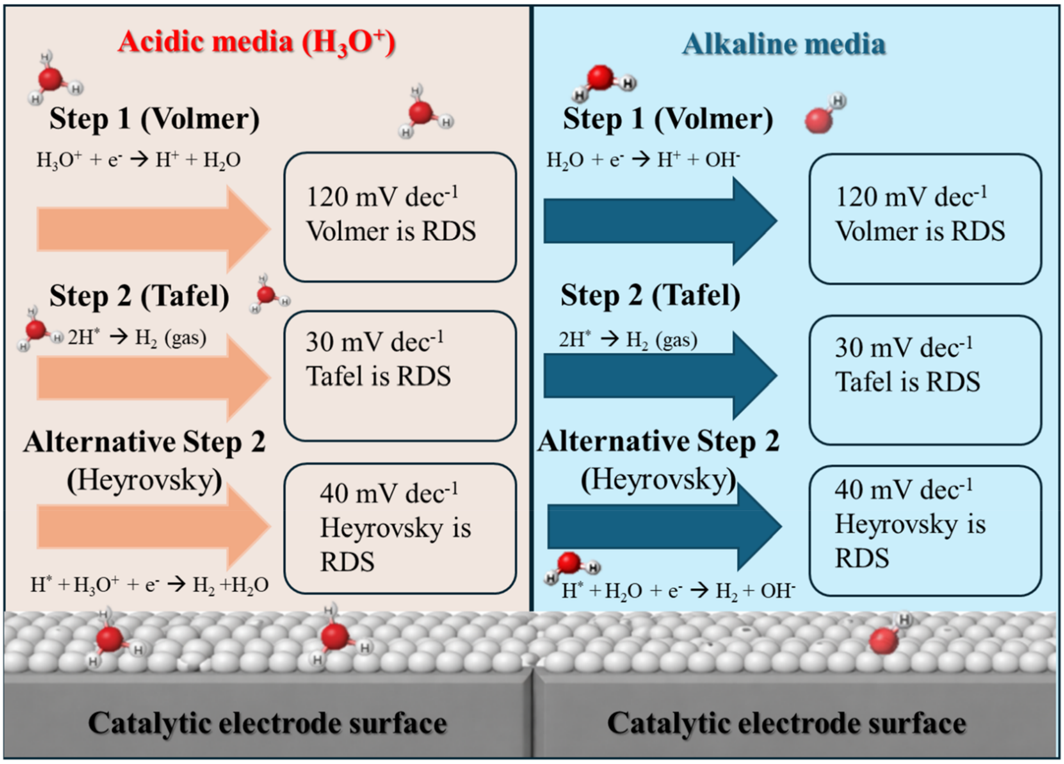

Fig. 2 Comparison of HER mechanisms and theoretical Tafel slopes.

values can vary depending on the catalyst structure, surface morphology, and experimental conditions, as will be mentioned afterwards.[38]

3. Key parameters for evaluating electrocatalytic performance in the hydrogen evolution reaction (HER)

Numerous parameters are employed to assess the catalytic performance of HER electrocatalysts. These parameters provide valuable insights into the reaction kinetics and thermodynamics. A concise overview of these evaluation criteria is schematically illustrated in Fig. 3 and further analyzed below.[26]

3.1. Overpotential (η)

Overpotential is a fundamental parameter for evaluating HER electrocatalysts. It represents the difference between the experimentally observed potential and the thermodynamically calculated equilibrium potential during an electrochemical reaction. Overpotential arises from various factors, including charge-carrier diffusion, activation energy barriers, and ohmic resistance. Conventionally, the overpotential required to achieve a current density of 10 mA cm^{-2} is used as a benchmark for comparing HER catalytic activity. This current density corresponds to a 12.3% solar-to-hydrogen efficiency.[39]

3.2. Tafel slope

The Tafel slope is derived from the linear region of the Tafel plot, typically obtained through linear sweep voltammetry (LSV). It is instrumental in analyzing the rate-determining step (RDS) of the HER mechanism, assuming a high surface coverage of adsorbed hydrogen (H_{ads}). Lower Tafel slope values indicate faster charge transfer kinetics at the electrode–electrolyte interface, reflecting superior catalytic behavior. The Tafel slope and exchange current density are key parameters used to evaluate the electrocatalytic activity of materials, particularly in the hydrogen evolution reaction (HER).[39] These parameters are derived from the Tafel equation:

$$\eta = a + b\log j, \tag{7}$$

where η is the overpotential, j is the current density, a is the intercept, and b is the Tafel slope. A Tafel plot, which graphs overpotential against the logarithm of current density, provides two critical kinetic insights: the Tafel slope and the exchange current density (j_0). The Tafel slope reflects the electron-transfer kinetics and is directly related to the underlying reaction mechanism. A lower Tafel slope indicates that a slight increase in overpotential results in a significant rise in current density, suggesting faster catalytic kinetics. On the other hand, the exchange current density represents the rate of charge transfer at equilibrium (zero overpotential) and serves as a measure of the intrinsic catalytic activity. A higher j_0 value implies a lower energy barrier for electron transfer and a more efficient catalyst. Thus, a high-performance electrocatalyst is typically characterized by a low Tafel slope and a high exchange current density, indicating both favorable reaction kinetics and vigorous intrinsic activity.[40,41]

3.3. Exchange current density (j_0)

Exchange current density refers to the current density at which the anodic and cathodic currents are equal under equilibrium

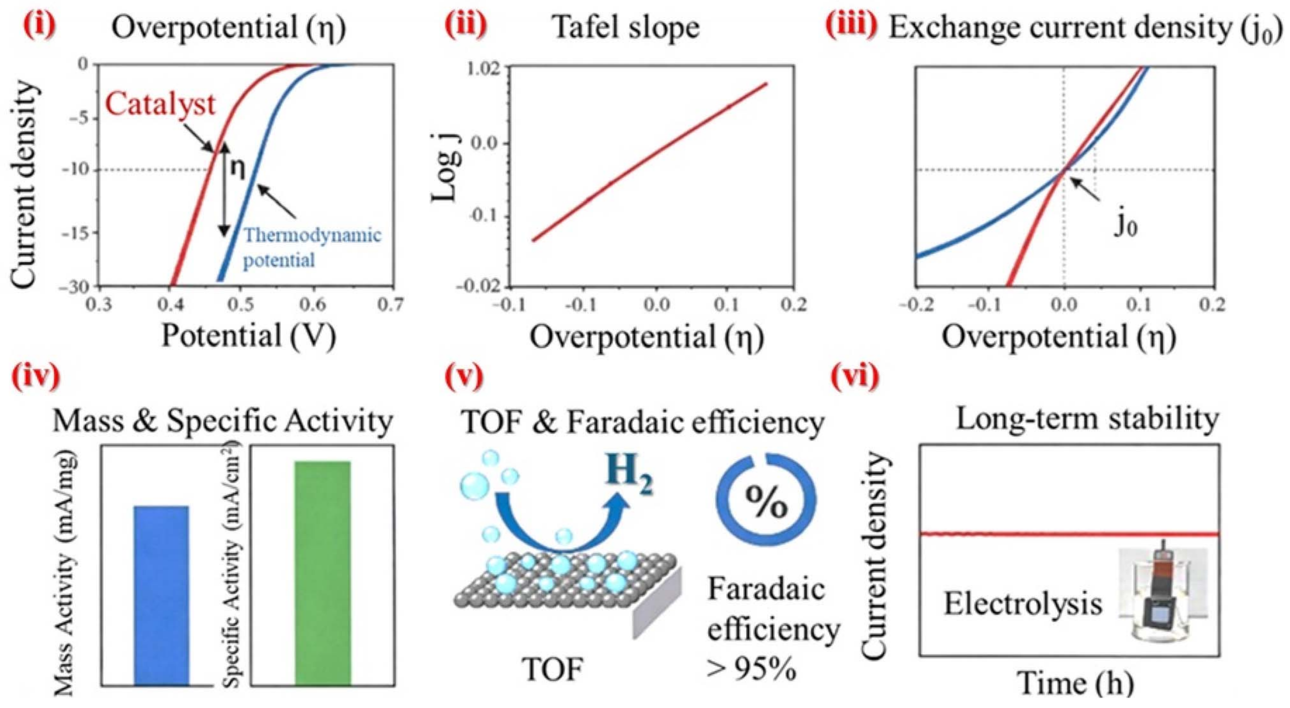

Fig. 3 Schematic overview of the key parameters used to evaluate the catalytic performance of HER electrocatalysts.

conditions. It is determined by extrapolating the linear portion of the Tafel plot to the *x*-axis. This parameter reflects the intrinsic charge-transfer activity between the electrode and the electrolyte. Higher exchange current densities indicate more efficient HER performance.[42]

3.4. Mass and specific activity

These parameters provide quantitative insights into electrocatalytic activity:

- Specific activity is defined as the current density normalized to the electrochemically active surface area (ECSA) or the Brunauer–Emmett–Teller (BET) surface area. It reflects the intrinsic activity of individual catalytic sites.[43]
- Mass activity normalizes the current output to the catalyst's loading mass. It primarily depends on the accessible surface area and is typically higher for catalysts with greater surface exposure.[43]

3.5. Turnover frequency (TOF) and faradaic efficiency

- TOF quantifies the number of hydrogen molecules generated per active site per second at a given potential. Although precise determination is challenging due to uncertainty in the number of true active sites, approximations are often made assuming full participation of surface atoms or based on mass loading.[44]
- Faradaic efficiency indicates the efficiency of charge conversion into hydrogen. It is calculated as the ratio of the actual amount of H_2 produced to the theoretical amount, which is derived using Faraday's laws of electrolysis. Practical measurements typically involve gas chromatography or water-displacement methods. A highly efficient catalyst approaches 100% faradaic efficiency.[22,45]

3.6. Long-term stability

The durability of electrocatalysts under prolonged operation is critical for real-world applications. Stability is typically assessed by:

- Chronopotentiometry, where the catalyst is subjected to a constant current density (commonly 10 mA cm^{-2} or 100 mA cm^{-2}) over extended periods, and changes in potential are monitored.
- Accelerated Cyclic Voltammetry (CV), involving repeated potential scans (often thousands of cycles), with performance degradation evaluated by comparing pre- and post-cycle polarization curves. A slight increase in overpotential after cycling indicates good long-term stability.

4. Advanced computational and characterization studies of Ni-based HER catalysts

While *in situ* and *operando* characterization techniques provide direct experimental evidence of surface reconstruction and phase evolution of Ni electrodes during the hydrogen evolution reaction (HER), computational modeling, particularly density functional theory (DFT), offers complementary atomistic insight into hydrogen adsorption energetics, interfacial charge transfer, and structure–activity relationships. The combined use of theoretical and experimental approaches is essential for identifying the actual catalytically active state of monometallic Ni under operating HER conditions.

DFT studies have demonstrated that HER activity on pristine Ni surfaces is governed primarily by hydrogen adsorption energetics. On Ni(111), the hydrogen adsorption free energy (ΔG_{H^*}) has been reported in the range of −0.25 to −0.35 eV, indicating stronger-than-optimal hydrogen binding relative to the thermoneutral value ($\Delta G_{H^*} = 0$ eV) and accounting for the comparatively sluggish HER kinetics of this facet.[46] Surface crystallography plays a decisive role, as Ni(100) and Ni(110) surfaces generally bind hydrogen more weakly than Ni(111), with ΔG_{H^*} values closer to zero, suggesting more favorable HER kinetics at undercoordinated sites.[47,48]

Beyond facet-dependent effects, both experimental models and DFT calculations demonstrate that interfacial engineering plays a decisive role in enhancing HER performance on monometallic Ni electrodes. This behavior is well captured by the chimney effect proposed for metal/oxide composite catalysts, in which strong electronic coupling at the oxide/Ni interface induces charge redistribution that selectively stabilizes adsorbed hydrogen intermediates (H*) while suppressing competing H_2O^* and OH* adsorption.[49] As schematically illustrated in Fig. 4 (adapted from Peng *et al.*), this interfacial environment creates an energetically favorable "chimney" for hydrogen evolution, in which H* formation and H_2 desorption occur preferentially at interfacial Ni sites. Consistent with this model, DFT calculations reveal that Ni/NiO heterointerfaces generate $Ni^{\delta+}$ centers that balance hydrogen adsorption strength and shift ΔG_{H^*} toward thermoneutral values, thereby lowering kinetic barriers for HER.[49,50]

Significantly, HER activity scales with the density of interfacial metal atoms, underscoring that even in nominally monometallic Ni electrodes, surface oxidation and metal/oxide heterojunctions are central determinants of catalytic performance.[49,50] This interfacial charge modulation lowers kinetic barriers and correlates well with experimentally observed

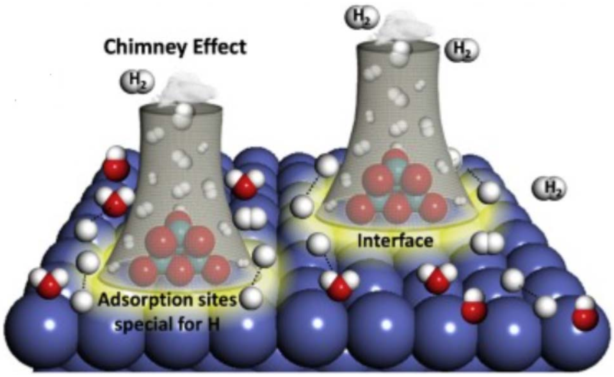

Fig. 4 Schematic illustration of the "chimney effect" at the Ni/oxide interface. Reprinted from L. Peng, *et al.*, copyright (2023), with permission from Elsevier.[49]

Table 1 DFT summary of hydrogen adsorption energetics and HER insights for Ni-based catalysts

Surface/interface	ΔG_{H^*} (eV)	DFT insights for HER	Ref.
Ni(111)	−0.25 to −0.35	Strong H binding; sluggish kinetics *vs.* Pt	47 and 48
Ni(100)	−0.10 to −0.20	Weaker H binding than Ni(111); closer to optimal	53
Ni(110)	−0.15	Moderate binding, undercoordinated sites enhance activity	54
Ni/NiO interface	0.0 to −0.05	Charge transfer balances adsorption; stabilizes active $Ni^{\delta+}$ sites	50
Hydroxylated Ni surface	Closer to 0 (tuned by OH groups)	Facilitates water dissociation, improves proton adsorption	51

reductions in Tafel slopes. In addition, DFT simulations indicate that hydroxylated Ni surfaces facilitate water dissociation and proton adsorption, in agreement with *operando* Raman and XPS observations identifying surface hydroxyl species as key contributors to alkaline HER activity.[51,52] These computational insights collectively demonstrate that pristine metallic Ni is intrinsically suboptimal for HER, whereas dynamically reconstructed surfaces and interfaces effectively tune adsorption energetics toward optimal values.

A summary of representative DFT-derived hydrogen adsorption energies and mechanistic insights for Ni-based HER catalysts is provided in Table 1, highlighting the critical role of surface orientation, interfacial charge transfer, and hydroxylation in governing catalytic performance.

Understanding the dynamic evolution of Ni surfaces under electrochemical bias is equally critical for rational catalyst design. Conventional *ex situ* characterization techniques often fail to capture transient intermediates and metastable active states formed during HER. To overcome these limitations, advanced *in situ* and *operando* techniques, including Raman spectroscopy, X-ray photoelectron spectroscopy (XPS), X-ray absorption spectroscopy (XAS), and electron microscopy, have been increasingly employed to probe Ni catalysts under realistic reaction conditions (Fig. 5).

In situ Raman spectroscopy has emerged as a powerful tool for monitoring surface transformations of Ni-based catalysts during HER. By enabling real-time observation of vibrational modes, Raman spectroscopy captures structural and chemical changes that occur under applied electrochemical bias.[55] Lai *et al.* employed *in situ* Raman spectroscopy to investigate Ni/$Ni(OH)_2$ heterostructures during alkaline HER, observing progressive intensification of Ni–O stretching modes in the 470–560 cm^{-1} range, confirming electrochemical hydroxylation of metallic Ni into $Ni(OH)_2$.[56] Notably, the study demonstrated that the Ni/$Ni(OH)_2$ interface serves as the accurate catalytic site, where hydroxyl species promote faster hydrogen adsorption and desorption (Fig. 6).

In addition, *operando* X-ray absorption spectroscopy (XAS) at the Ni K-edge provides quantitative insight into changes in the local electronic structure and coordination environment, capturing reversible transitions between Ni^0 and Ni^{2+} states during electrocatalysis. These *operando* observations demonstrate that metallic Ni undergoes dynamic surface oxidation under applied bias, forming thin NiO/$Ni(OH)_2$ layers that coexist with subsurface Ni^0. The persistence of these oxidized

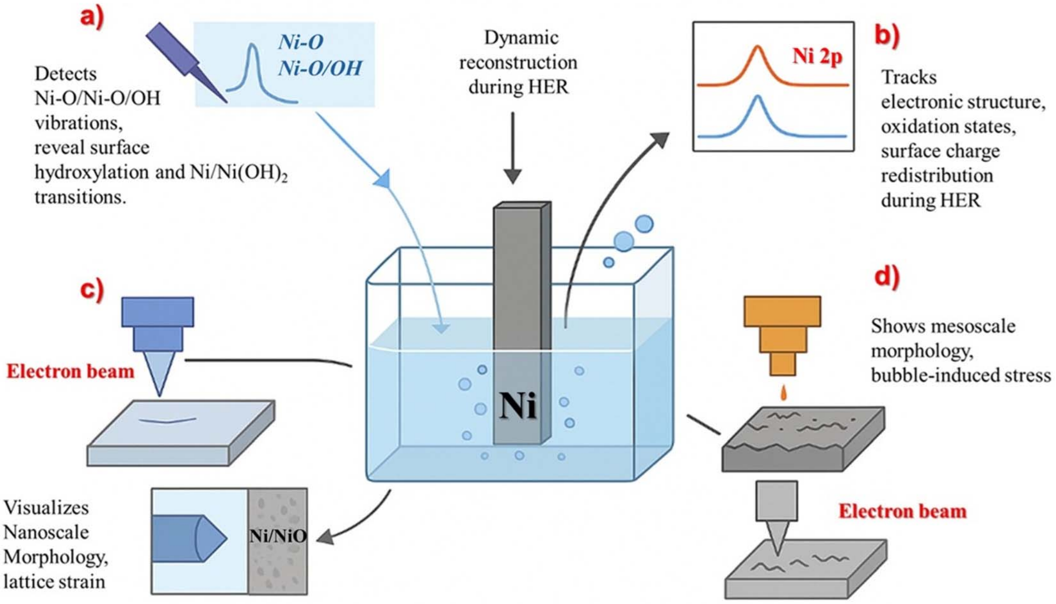

Fig. 5 *Operando* techniques applied for characterization of Ni-based electrodes: Raman (a), XPS (b), TEM (c) and SEM (d).

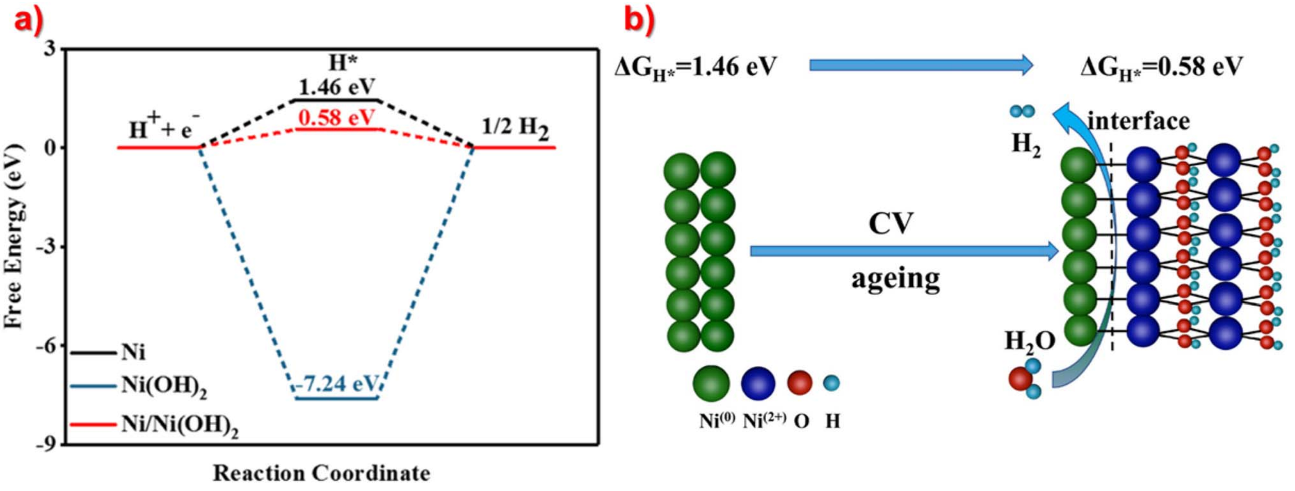

Fig. 6 Calculated free energy for atomic hydrogen adsorption on Ni, $Ni(OH)_2$, and $Ni/Ni(OH)_2$ and proposed mechanism for the enhanced HER on $Ni/Ni(OH)_2$ heterostructure. Reprinted from W. Lai, *et al.*, copyright (2021), with permission from Elsevier.[56]

motifs during operation highlights their role in modulating hydrogen adsorption energetics and interfacial charge transfer, underscoring the importance of *operando* characterization in identifying the catalytically relevant states of Ni-based HER electrode.[57]

Also, recent shell-isolated nanoparticles enhanced Raman spectroscopy (SHINERS) studies have revealed the dynamic formation and interconversion of α-$Ni(OH)_2$, β-$Ni(OH)_2$, and Ni(O)OH species on nickel surfaces under alkaline polarization, providing direct spectroscopic evidence of surface reconstruction processes that are not discernible from electrochemical measurements alone.[58] While metallic Ni persists beneath these layers, the coexistence of surface-bound oxide and hydroxide motifs highlights the complex interfacial environment present under operating conditions and underscores the importance of *operando* spectroscopy in identifying catalytically relevant surface states in Ni-based electrocatalysts.[58]

In a similar manner, near-ambient-pressure XPS (NAP-XPS) complements Raman spectroscopy by providing electronic and chemical-state information under reaction-relevant conditions. *Operando* XPS studies reveal reversible transformations between metallic Ni^0 and oxidized Ni^{2+} states during HER, accompanied by surface hydroxylation and the formation of $Ni^{\delta+}$ species. Thurner *et al.* demonstrated potential-dependent oscillations between Ni^0 and Ni^{2+} on patterned Ni electrodes, directly correlating electronic reconstruction with HER activity.[59] Similarly, Liu *et al.* reported shifts in Ni 2p binding energies during alkaline HER, reflecting electronic structure modulation induced by OH^- adsorption.[60]

In situ electron microscopy provides direct visualization of Ni catalyst restructuring across multiple length scales. Liquid-phase TEM and cryo-TEM studies have captured nanoparticle nucleation, attachment, and interfacial fusion processes in real time, confirming the formation of metastable Ni/NiO interfaces that function as HER-active sites.[61,62] Complementary *in situ* SEM observations reveal the impact of gas evolution, in which hydrogen bubble formation induces stress, cracking, and the exposure of new catalytic sites.[63] Together, these techniques demonstrate that Ni HER activity arises from continuously

Table 2 Comparative overview of *in situ* and *operando* characterization techniques for Ni-based HER catalysts

Technique	What it probes	Key insights for Ni-HER	Ref.
In situ Raman spectroscopy	Vibrational modes of Ni–O, Ni–OH, and adsorbed H* intermediates	Confirms dynamic Ni → $Ni(OH)_2$/NiOOH transformations; $Ni/Ni(OH)_2$ interface is the active site	56 and 57
In situ XPS (NAP-XPS)	Oxidation states (Ni^0, Ni^{2+}, $Ni^{\delta+}$), electronic structure, hydroxylation	Shows reversible redox transitions, electronic modulation by OH^-, formation of $Ni^{\delta+}$ centers	59 and 60
In situ TEM	Atomic/nanoscale morphology, lattice strain, nucleation, phase transformation	Direct visualization of restructuring, nanoparticle attachment, Ni/NiO interface stability	61 and 62
In situ SEM	Surface morphology, bubble formation, catalyst cracking under HER bias	Reveals mesoscale effects of gas evolution, stress-induced cracking, and exposure of new active sites	63

evolving surface and interfacial structures rather than static pristine phases.

A comparative overview of the capabilities and insights provided by these *in situ* and *operando* techniques is summarized in Table 2.

5. Fine-tuning engineering strategies for enhancing HER performance of monometallic nickel electrodes

The hydrogen evolution activity of monometallic nickel (Ni) can be markedly enhanced through rationally designed engineering strategies that modulate its surface chemistry, interfacial electronic configuration, structural morphology, and crystallographic defect architecture. Fig. 7 shows that each of these parameters decisively influences the fundamental steps of the HER: water dissociation, proton adsorption, and molecular hydrogen desorption. By tuning the local electronic density and coordination of Ni active sites, these strategies can optimize the hydrogen adsorption free energy (ΔG_{H^*}), facilitate charge-transfer kinetics at the electrode–electrolyte interface, and stabilize the catalytically active phase under sustained operation.[64] Beyond improving intrinsic activity, such fine-tuning approaches enhance mass transport, mitigate bubble accumulation, and suppress degradation pathways such as surface oxidation or nanoparticle agglomeration.[65] Together, they establish a versatile design toolbox for tailoring monometallic Ni toward high efficiency, long-term stability, and industrially relevant current densities in alkaline electrolysis. The following subsections detail the fundamental concepts and representative progress associated with each major strategy class.

5.1. Surface modification

Surface modification is among the most direct and versatile approaches to enhancing the hydrogen-evolution activity of nickel electrodes. It involves the deliberate tailoring of the outermost atomic layers, through oxidation, hydroxylation, plasma activation, or laser-induced restructuring, to optimize the surface electronic structure and catalytic site chemistry without fundamentally altering the bulk phase.[15,16,66] The catalytic behavior of Ni is intimately governed by the binding

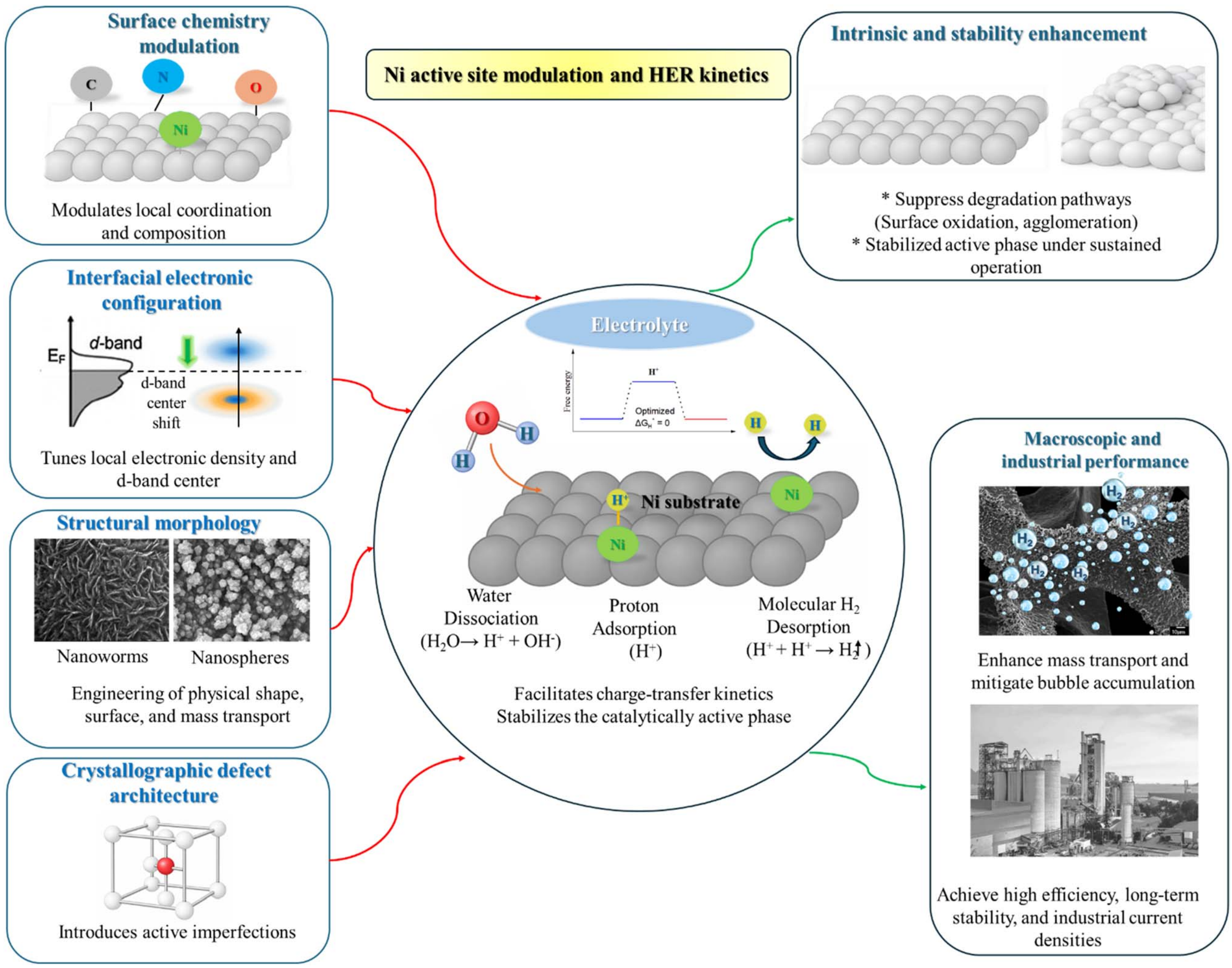

Fig. 7 Schematic overview of fine-tuning engineering strategies for enhancing the HER performance of monometallic nickel-based electrodes.

strength of hydrogen intermediates (H*), quantified by the adsorption free energy (ΔG_{H^*}). On pristine Ni surfaces, ΔG_{H^*} tends to be slightly negative (~ -0.25 to -0.35 eV), indicating robust H binding that slows desorption.[67] Controlled surface modification can partially oxidize Ni atoms into $Ni^{\delta+}$ states or generate Ni–O/Ni–OH species, thereby tuning the d-band center and shifting ΔG_{H^*} toward the thermoneutral regime.[22,68] These altered sites facilitate both the Volmer step (water dissociation) and subsequent Heyrovsky/Tafel steps (Fig. 1), thereby accelerating hydrogen evolution kinetics, particularly under alkaline conditions.

Beyond purely electronic effects, surface modification can also reshape the micro- and nanoscale topography, increasing the electrochemically active surface area (ECSA) and promoting more efficient bubble detachment. As highlighted by Prabhu and Lee, topographically disordered surfaces containing steps, kinks, vacancies, and strained atomic environments exhibit enhanced catalytic activity due to lowered activation barriers for adsorbate formation and migration.[69] Their conceptual framework emphasizes how deviations from ideal crystalline order increase the density of highly active, low-coordination metal sites. Unlike flat, low-index planes where active sites are geometrically limited, these disordered topographies maximize the exposure of catalytically potent atoms. When applied to modified Ni electrodes, this strategy effectively activates the basal planes, creating a surface landscape where reactants can readily adsorb and dissociate, thereby bypassing the limitations imposed by thermodynamic equilibrium phases.

Recent literature provides compelling evidence that deliberate surface engineering of nickel can substantially elevate its intrinsic hydrogen evolution reaction (HER) activity and long-term stability in alkaline media, primarily by tuning the electronic structure and interfacial chemistry of surface Ni sites. One representative strategy is heterointerface formation between metallic Ni and its derived phases, exemplified by the Ni_3N/Ni heterostructure reported by Xiong *et al.*[70] In this system, *in situ* phase separation during surface thermal nitridation creates abundant Ni_3N/Ni interfaces with strong electronic coupling. Spectroscopic analysis and DFT calculations reveal electron transfer from metallic Ni to Ni_3N at the heterointerface, generating electronically modified interfacial Ni sites with optimized hydrogen-adsorption energetics. As a result, the Ni_3N/Ni electrode achieves a low overpotential of 144 mV at 10 mA cm^{-2} and a reduced Tafel slope (107 mV dec^{-1}), markedly outperforming either pure Ni or pure Ni_3N. Notably, the catalyst exhibits exceptional durability, with only a $\sim$14 mV increase in overpotential after 6000 cycles and stable operation at high current densities, underscoring the stabilizing role of interfacial electronic reconstruction.

Complementary insights are provided by surface strain engineering at Ni/NiO interfaces, as demonstrated by Yi *et al.*[71] By selectively oxidizing or reducing the surface of Ni and NiO, the authors induced lattice-mismatch-driven compressive or tensile strain in the surface Ni layers. DFT analysis shows that compressive strain on surface Ni (in surface-reduced NiO, sr-NiO) downshifts the Ni d-band center, weakening overly strong H adsorption and facilitating H_2 desorption, identified as the rate-limiting step on metallic Ni. Experimentally, this strain-engineered sr-NiO electrode exhibits a significantly lower overpotential of 164 mV at 10 mA cm^{-2} and superior stability compared with surface-oxidized Ni ($\eta_{10} = 565$ mV), with minimal degradation over 50 h of continuous operation. These results directly link surface lattice distortion, electronic structure modulation, and enhanced HER kinetics.

A key insight emerging from recent studies is that Ni surfaces are not static under HER conditions but undergo electrochemically induced self-reconstruction. *Operando* and *in situ* analyses demonstrate that metallic Ni readily transforms into thin layers of $Ni(OH)_2$ or NiOOH during polarization, even under cathodic bias. Meng *et al.*,[72] and Kumaravel *et al.*[73] showed that such reconstruction processes dynamically alter surface chemistry, creating catalytically competent $Ni^{\delta+}$–OH sites. While much of this work focuses on oxygen evolution, the same reconstruction phenomena are increasingly recognized as relevant to HER-active Ni electrodes. Direct experimental evidence for this transformation under HER conditions is provided by *in situ* Raman spectroscopy. Lai *et al.*[56] monitored the evolution of Ni/$Ni(OH)_2$ surfaces during HER and observed a progressive increase in Ni–O stretching modes between $\sim$470 and 560 cm^{-1}, indicating surface hydroxylation and the formation of catalytically active Ni–OH species.

Beyond chemical modification, advanced physical surface-engineering techniques have proven highly effective for optimizing Ni electrodes. Laser-based approaches – including laser-induced material transfer, femtosecond laser ablation, and laser nanostructuring – can generate hierarchical micro- and nano-scale surface features, introduce localized strain, and increase surface roughness without changing bulk composition. The comprehensive review by Lee *et al.*[66] provides an overview of laser-induced surface functionalization strategies, while Ma *et al.*[74] demonstrated that 3D-ordered Ni surface architectures dramatically improve gas bubble detachment and sustain high current densities during alkaline water electrolysis. These modifications substantially enhance bubble-release dynamics and reduce overpotentials to below 120 mV at 10 mA cm^{-2}.[15,41,74] Complementary strategies such as plasma treatment, chemical etching, and electrodeposition on pre-structured substrates further expand the surface design toolbox. For instance, in our previous work,[40] we showed that electrodepositing Ni particles onto laser-nanostructured Ni substrates produced a synergistic increase in roughness, wettability, and active-site density, leading to significantly reduced HER overpotentials ($\eta_{10} = 108$ mV).[40] The comparative surface-morphology images in Fig. 8 clearly demonstrate the impact of laser nanostructuring on the local surface structure, which in turn results in enhanced active-site density and improved HER performance.

Consistent with these observations, laser-engineered Ni surfaces routinely deliver HER overpotentials below 108 mV at 10 mA cm^{-2},[40] with Tafel slopes as low as 88 mV dec^{-1},[75] metrics that overlap with, and in some cases rival, those reported for widely studied multicomponent systems such as Ni–Mo and Ni–Fe alloys (Table 4).[76,77] Crucially, these performances are achieved without compositional modification, demonstrating that

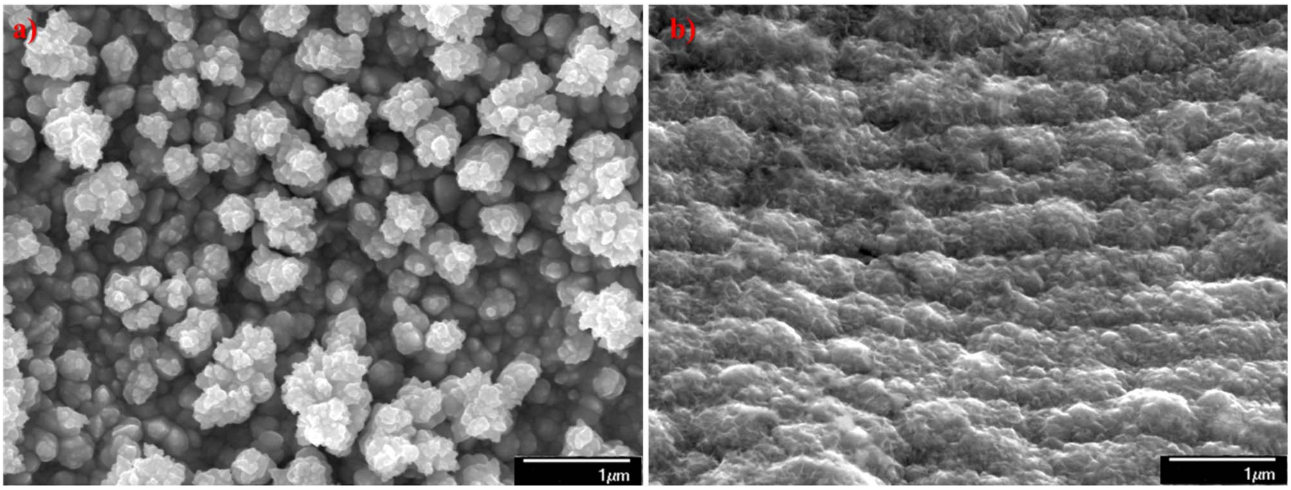

Fig. 8 Ni electrodeposition on (a) untreated Ni sheet, (b) laser nanostructured Ni sheet. Reprinted from I. Poimenidis, *et al.*, copyright (2022), with permission from Elsevier.[40]

deliberate surface structuring through controlled roughening, wettability enhancement, and exposure of undercoordinated Ni sites can elevate monometallic Ni into the activity window of state-of-the-art alkaline HER electrocatalysts. These results underscore that advanced surface modification, rather than alloying or doping, can be sufficient to approach Pt-group benchmarks under alkaline conditions and to achieve competitive HER behavior in Ni-based electrodes (Table 4).[16,40,78]

5.2. Interface engineering

Interface engineering represents a more sophisticated extension of surface modification, in which the boundary region between distinct phases or domains, such as Ni/NiO, Ni/Ni$(OH)_2$, Ni/carbon, or Ni/polymer composites, is intentionally engineered to manipulate local electronic structure and catalytic function. The primary objective of this strategy is to harness synergistic charge redistribution between dissimilar phases to overcome the intrinsic kinetic limitations of monometallic catalysts. Beyond activity enhancement, well-designed interfaces also improve durability by suppressing corrosion, inhibiting nanoparticle sintering, and stabilizing active phases under dynamic operating conditions.[79]

In the case of Ni/NiO and Ni/Ni$(OH)_2$ interfaces, systematic experimental and theoretical analysis by Neumüller *et al.* demonstrates that partial surface oxidation of metallic Ni leads to the coexistence of Ni^0, NiO, and Ni$(OH)_2$ domains, forming abundant metal/oxide and metal/hydroxide junctions without significant changes in surface roughness.[80] XPS and electrochemical measurements reveal that these interfaces increase the intrinsic HER exchange current density by a factor of 3–5, confirming that activity enhancement originates from interfacial electronic effects rather than geometric surface area. Specifically, at Ni/NiO and Ni/Ni$(OH)_2$ boundaries, differences in electronegativity and coordination generate electronically polarized interfacial regions, as schematically illustrated in Fig. 9. Computational analysis indicates that oxide-modified Ni interfaces selectively modulate adsorbate binding behavior relative to pristine Ni surfaces, consistent with the interfacial reaction pathways (Fig. 9). Multiscale simulations further reveal that interfacial regions act as spatially localized activity centers that influence hydrogen coverage and utilization across adjacent metallic domains. Although bulk NiO and Ni$(OH)_2$ phases are intrinsically less active for HER, their intimate coupling with metallic Ni creates functionally differentiated interfacial domains in which complementary adsorption and reaction roles are spatially distributed, enabling sustained catalytic turnover.[80] Notably, simulations reveal an optimal oxide coverage, beyond which excessive oxidation reduces the density of contiguous Ni sites and suppresses HER activity, underscoring the need for precise control over interfacial density and continuity.[80]

A classic manifestation of these principles is the Ni/NiO heterostructure, widely reported as an archetype of self-adaptive HER catalysts.[81–83] Controlled oxidation of metallic Ni, followed by mild reduction or electrochemical activation, produces nanoscale junctions where electronic coupling at the Ni–O interface enhances the local charge density on surface Ni atoms. As a result, Ni/NiO heterostructures fabricated *via* controlled oxidation–reduction or solvothermal routes exhibit overpotentials of 110–140 mV, and Tafel slopes of 86 mV dec^{-1}, narrowing the activity gap with Pt-group metals in alkaline media[50,84] (Table 4).

Such improved activity has been attributed, at least in part, to a possible bifunctional catalytic mechanism at Ni/NiO or Ni/Ni$(OH)_2$ interfaces. In this mechanism, hydroxylated oxide domains preferentially adsorb OH* species generated during water dissociation, while adjacent metallic Ni sites stabilize hydrogen intermediates (H*), facilitating their recombination into H_2. Similar bifunctional pathways have been proposed for HER catalysts such as Pt–Ru systems, highlighting the importance of oxide–metal interfaces in accelerating alkaline HER kinetics.[85] Also, recent studies further support this interpretation by demonstrating that Ni/Ni$(OH)_2$ interfaces enhance

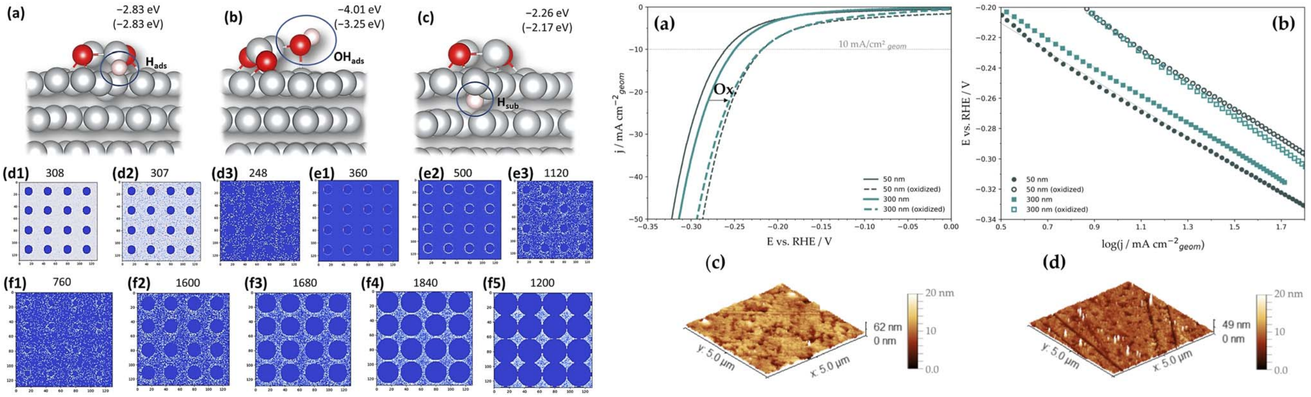

Fig. 9 Schematic illustration of functionally differentiated domains at Ni/NiO and Ni/Ni(OH)$_2$ interfaces under alkaline HER conditions.[80] Left: DFT and KMC modeling of an oxide-modified Ni catalyst surface (a) optimized structure of H$_{ads}$ on (NiO)$_2$@Ni(111), (b) optimized structure of OH$_{ads}$ on (NiO)$_2$@Ni(111), and (c) subsurface H (H$_{sub}$) in (NiO)$_2$@Ni(111). Right: (a) HER polarization curves before and after oxidation, (b) Tafel plots, (c) AFM image of a 50 nm-thick film after cycling to anodic potentials, (d) AFM image of a 300 nm-thick film after cycling to anodic potentials.

alkaline HER kinetics by promoting water adsorption and dissociation on hydroxide domains, while hydrogen evolution occurs on adjacent metallic Ni sites, reinforcing the bifunctional role of oxide–metal junctions in nickel-based catalysts.[86]

Nickel–carbon (Ni/C) interfaces have also been demonstrated as an effective platform for enhancing alkaline hydrogen evolution reaction (HER) activity by combining the intrinsic catalytic properties of metallic Ni with the high electrical conductivity and large surface area of carbon supports.[87,88] Graphene- and carbon black-supported Ni catalysts exhibit substantially reduced overpotentials and Tafel slopes compared to bare Ni or carbon alone, reflecting accelerated reaction kinetics and improved interfacial charge transfer.[88] Structural and spectroscopic characterizations confirm that carbon substrates promote uniform dispersion and size confinement of Ni nanoparticles, suppress aggregation, and increase the electrochemically active surface area, thereby maximizing the utilization of Ni active sites.[87,88] Electrochemical impedance

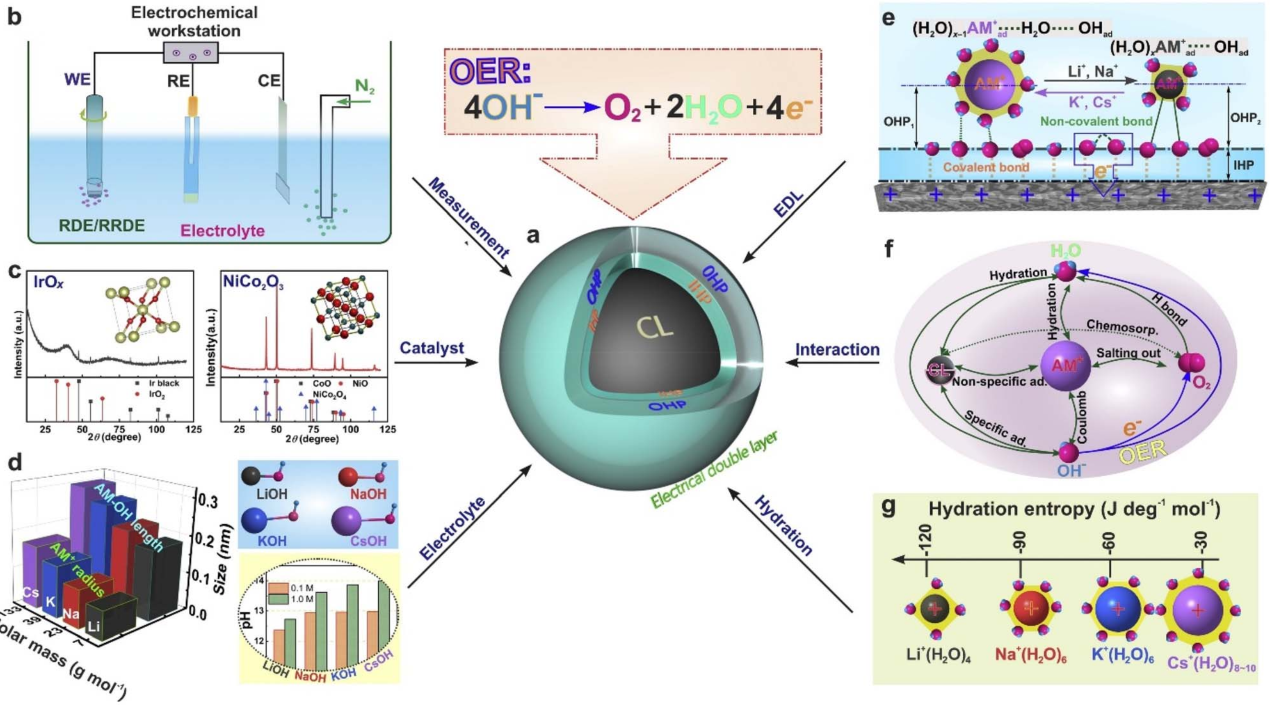

Fig. 10 Schematic illustration of the electric double layer (EDL) in alkaline media, highlighting the distribution of solvated cations (AM$^+$), hydroxide species, and interfacial water molecules. The interaction between hydrated cations and adsorbed hydroxyl species (OH*) at the outer Helmholtz plane influences the local electric field and hydrogen-bond network, thereby modulating water dissociation and HER kinetics. J. A. D. del Rosario, *et al.*, copyright (2021), with permission from Elsevier.[92]

spectroscopy further reveals that the Ni/C interface significantly lowers charge-transfer resistance, underscoring the role of the carbon matrix in facilitating rapid electron transport between Ni active sites and the electrolyte.[87] From a mechanistic perspective, the synergistic interaction at the Ni/C interface optimizes hydrogen adsorption energetics ($\Delta G_{\mathrm{H}*}$), enabling efficient Volmer–Heyrovsky pathways in alkaline media, while the carbon support stabilizes Ni nanoparticles and ensures durable HER performance under prolonged operation.[88]

While the intrinsic catalytic properties of nickel surfaces play a central role in governing HER kinetics, the interfacial electrochemical environment can also significantly influence the reaction pathway. In particular, the structure of the electric double layer (EDL) at the electrode–electrolyte interface has recently emerged as a key factor affecting alkaline HER activity.[89,90] Because the Volmer step involves water adsorption and dissociation at the catalyst surface, the orientation of interfacial water molecules and the distribution of solvated cations within the EDL can strongly influence the energy barrier of this step[90–92] (Fig. 10). Recent studies have shown that tailoring the EDL through electrolyte composition or electrode surface structure can modify the local electric field and interfacial hydrogen-bond network, thereby facilitating water dissociation and hydrogen adsorption.[91,93] Consequently, rational engineering of the EDL is increasingly recognized as a complementary strategy that can facilitate water dissociation kinetics in nickel-based electrocatalysts. A schematic representation of the EDL structure and its influence on interfacial water organization and cation distribution is shown in Fig. 10.

5.3. Morphology control

The morphology of an electrocatalyst, encompassing its geometric configuration, dimensionality, and hierarchical architecture, plays a decisive role in determining its hydrogen-evolution performance. While the intrinsic electronic structure of nickel determines its catalytic nature, the spatial arrangement of atoms, crystallographic facets, and accessible voids dictates the number and utilization efficiency of active sites. By designing nickel into nanostructures with tailored shapes and rough surfaces, it is possible to simultaneously maximize the electrochemically active surface area (ECSA), optimize mass and electron transport, and facilitate gas bubble detachment during operation.

Morphologies such as nanoworms, nanowires, nanocones, and nanoparticles (Fig. 11), as well as generally porous structures, have been widely employed to optimize catalytic efficiency.[16,22,94–96] Three-dimensional (3D) architectures, such as NiO supported on nickel foam (NiO/NF), provide abundant active sites and superior electron transport pathways, enhancing overall catalytic performance.[94,97] In addition, protrusions created by Laser-Induced Periodic Surface Structures (LIPSS) have been found to enhance HER efficiency.[16] Such morphological engineering not only boosts catalytic activity but also supports long-term stability by facilitating efficient mass and electron transfer during electrolysis.

Nanostructured Ni surfaces typically display a morphology-dependent hydrogen utilization sequence, initiating at undercoordinated edges and corners before progressing to (111)

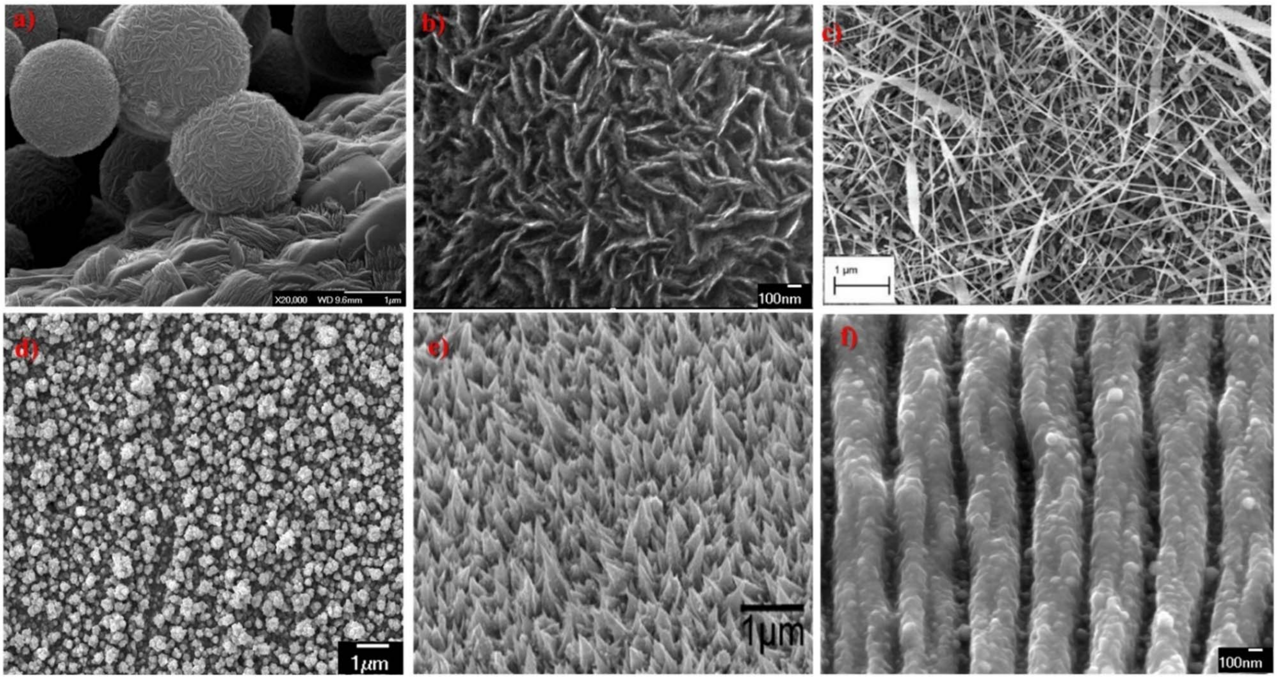

Fig. 11 Various Ni-based morphologies: nanoworms (a and b),[22] nanowires (c),[95] nanoparticles (d), nanocones (e),[94] protrusions (f).[16] Reprinted from I. Poimenidis, *et al.*, copyright (2023), with permission from Elsevier (a and b).[22] Reprinted from N. Kaur, *et al.*, copyright (2015), with permission from Elsevier (c).[95] Reprinted from Z. Du, *et al.*, copyright (2011), with permission from Elsevier (e).[94] Reprinted from I. A. Poimenidis, *et al.*, copyright (2021), with permission from Elsevier (f).[16]

facets and finally broad terrace sites at higher coverage.[98] These low-coordination and high-curvature features generate localized electronic and structural perturbations that differentiate hydrogen-binding behavior across the nanostructure, consistent with computationally predicted adsorption-energy variations of several tens of meV. The preferential participation of (111) facets reflects their greater structural compliance and ability to accommodate hydrogen without excessive lattice strain, in contrast to more rigid (100) terraces. At the nanoscale, the resulting spatial redistribution of surface hydrogen across distinct morphological domains promotes efficient hydrogen evolution and desorption while mitigating bubble accumulation, thereby enhancing the effective turnover frequency and faradaic efficiency. Collectively, the morphology-driven pathway depicted in Fig. 12 highlights that nanostructuring Ni extends beyond geometric surface-area enhancement and enables functional differentiation of surface sites that translates into improved HER performance.[99,100]

In summary, morphology-engineered Ni structures such as nanoworms, nanowires, porous Ni foams, and hierarchical Ni films achieve HER overpotentials of 45–180 mV and Tafel slopes as low as 80–111 mV dec^{-1}. These values overlap directly with those reported for multicomponent Ni-based catalysts, confirming that optimized Ni morphology alone can deliver state-of-the-art alkaline HER activity (Table 4).

5.4. Defect engineering

Defect engineering, particularly the deliberate introduction of lattice defects such as oxygen vacancies, has gained significant attention as a powerful tool to enhance the electrocatalytic performance of nickel monometallic electrodes for the HER. These structural imperfections can profoundly alter the electronic structure, surface chemistry, and reaction kinetics.[97] This electron enrichment increases progressively as the second and third oxygen vacancies are created. As a result, while the overall and individual oxygen atoms become increasingly electron-deficient, the total and individual nickel atoms gain electron density, reflecting a redistribution of charge within the NiO lattice driven by the vacancy-induced structural distortion (Fig. 13).[101] Moreover, oxygen vacancies can break the local lattice symmetry and induce localized states near the Fermi level, thereby increasing electrical conductivity and catalytic site accessibility.[102]

Several synthesis and post-treatment methods have been employed to introduce such defects. Controlled oxidation–reduction cycles, hydrogen annealing, and argon plasma treatment are among the most common approaches to generate oxygen vacancies. For example, hydrogen treatment of $Ni(OH)_2$ or NiO can partially reduce the material, forming oxygen-deficient NiO_x, which exhibits significantly improved HER activity due to enhanced conductivity and modified d-band

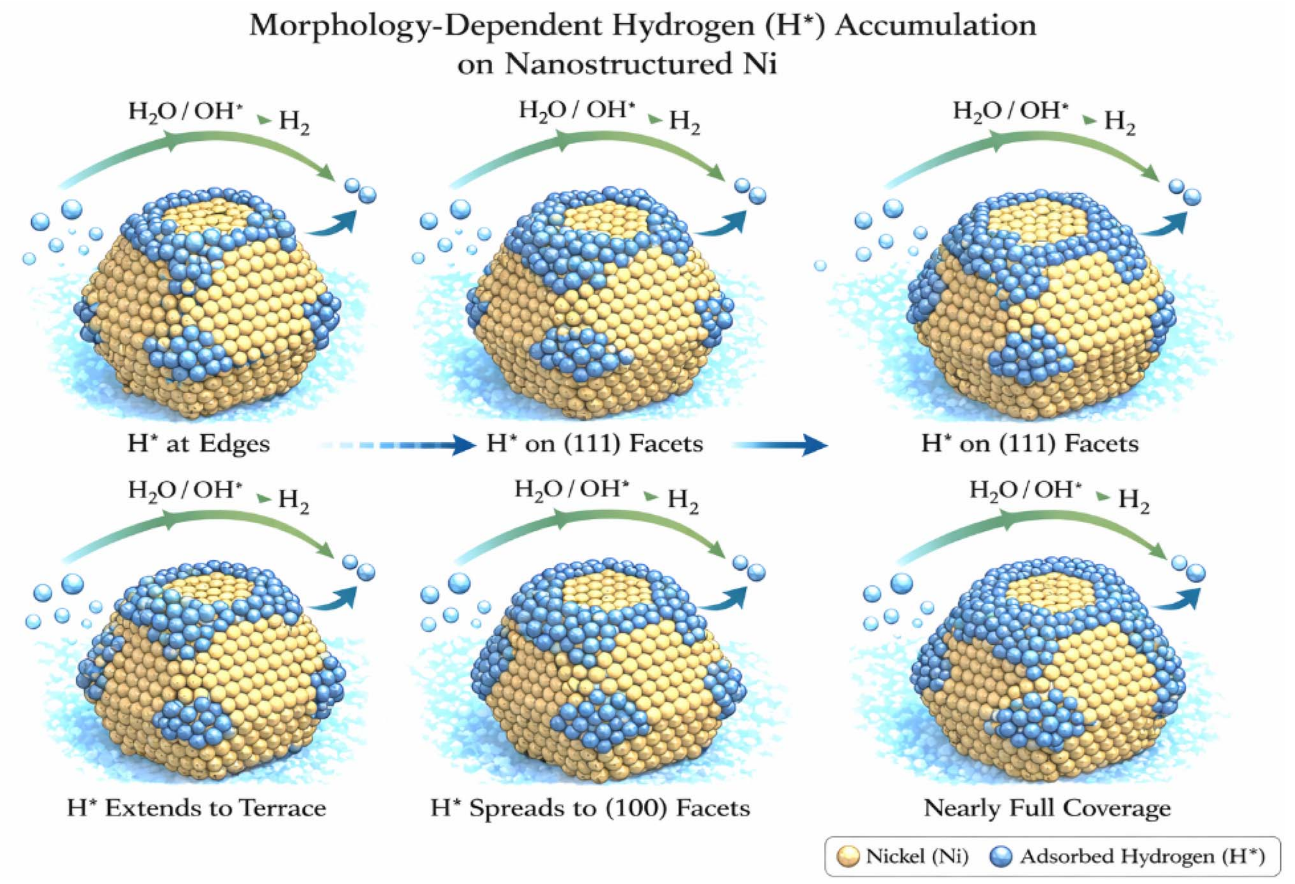

Fig. 12 Morphology-dependent hydrogen utilization pathways on nanostructured Ni electrodes.[99]

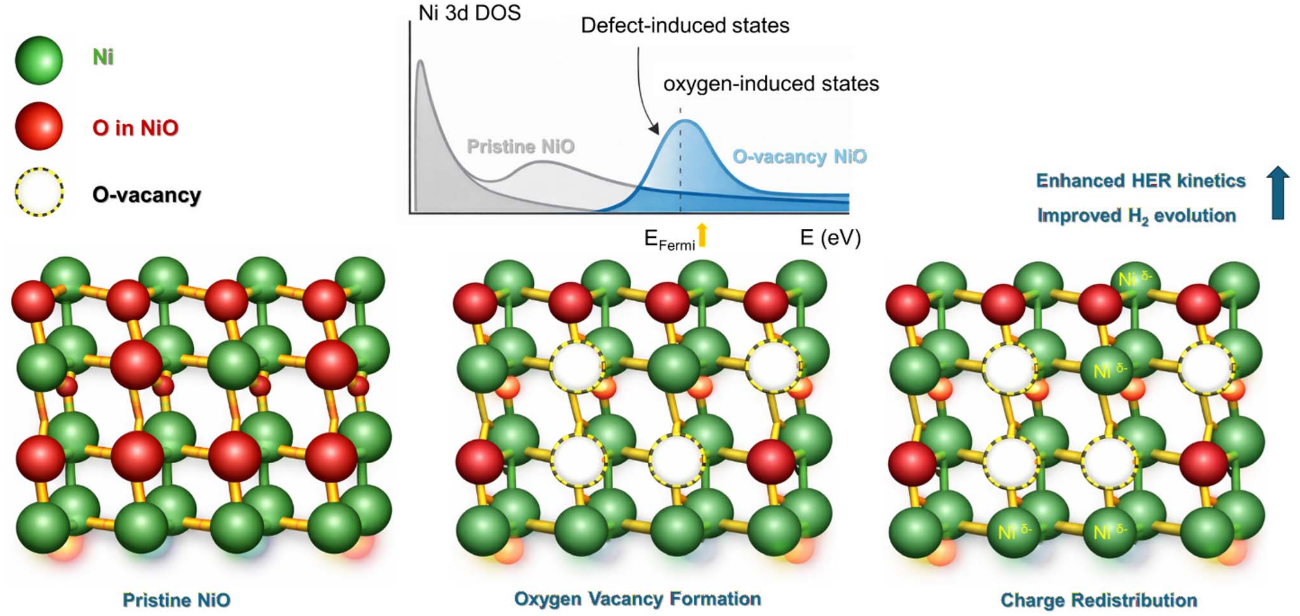

Fig. 13 Schematic representation of the Ni 3d density of states (DOS) for pristine NiO and oxygen-deficient NiO with oxygen vacancies and charge redistribution. Adapted conceptually from ref. 101 and 103.

centers.[104] Sonication, as shown in recent studies, not only changes the oxidation state of nickel species but also promotes the formation of defect-rich nanostructures with higher electrochemical surface areas.[105]

Cation vacancies (*e.g.*, Ni vacancies), dislocations, and grain boundaries have been reported to serve as catalytically active regions by tuning the local coordination environment and facilitating water adsorption and splitting.[106] Additionally, introducing strain or phase boundaries, such as between Ni and NiO or between amorphous and crystalline domains, can further amplify HER performance. For instance, Ni/NiO heterostructures with engineered defects show superior performance due to interfacial charge redistribution and synergistic effects between metallic and oxide phases (Fig. 13).[103]

In light of the above, Table 3 summarizes these fine-tuning strategies and their impact on key physicochemical properties. To quantify their effect on HER performance, Table 4 presents the electrocatalytic efficiency (Tafel slope and overpotential) of representative monometallic Ni electrodes developed *via* these methods. State-of-the-art multi-metallic Ni-based electrodes and noble-metal benchmarks are included for comparison. Notably, the data indicate that optimized monometallic electrodes can outperform multicomponent systems, closely approaching the efficiency of the benchmark Pt/C electrode.

It is worth noting that the combined application of surface modification, interface engineering, morphology control, and defect engineering enables the design of monometallic Ni electrodes with improved performance. When surface chemistry, interfacial structure, morphology, and defect density are co-optimized, the individual benefits of each strategy become mutually reinforcing, yielding nonlinear performance gains. For instance, surface modification (partial oxidation, hydroxylation, or carbon/graphene coating) establishes chemically active sites for water dissociation and regulates surface wettability, while interface engineering (*e.g.*, Ni/NiO or Ni/oxide–carbon junctions) creates charge-redistributed regions that decouple the Volmer and H–H recombination steps. As demonstrated in hollow Ni/NiO/C architectures derived from MOF precursors, the intimate coexistence of metallic Ni and defective NiO at the nanoscale enables efficient H–OH bond cleavage on oxide domains followed by rapid hydrogen recombination on adjacent metallic Ni sites, substantially lowering both overpotential and charge-transfer resistance[84] (Table 4).

Simultaneously, morphology control (hollow structures, hierarchical porosity, 3D foams) maximizes electrochemically active surface area, shortens electron/ion diffusion pathways, and facilitates bubble release, while defect engineering (Ni vacancies, oxygen vacancies, edge defects, oxygen functional groups) further enhances intrinsic activity by creating high-energy adsorption sites and alternative hydrogen spillover pathways. The GO-coated Ni foam system illustrates this synergy clearly: oxygen functional groups and structural defects in the carbon overlayer not only protect Ni from corrosion but also participate directly in HER kinetics by enabling proton transfer and hydrogen recombination at the Ni–carbon interface, resulting in a low overpotential of 83 mV at 10 mA cm^{-2} with a Tafel slope of 55.7 mV dec^{-1} (ref. 107) (Table 4).

In summary, the path toward next-generation earth-abundant Ni catalysts lies in the convergence of surface, interface, morphological, and defect engineering into unified architectures, supported by rigorous mechanistic understanding and reliable scaling strategies. Translating these design principles into functional Ni-based HER electrodes ultimately depends on the availability of versatile and

Table 3 Overview of the different fine-tuning engineering strategies for monometallic Ni HER electrocatalysts and their implications on key physicochemical properties

Strategy	Representative system	Engineered feature	Implications	Ref.
Surface modification	Ni → $Ni(OH)_2$/NiOOH	Surface oxidation/hydroxylation	Increased surface polarity and adsorption-site diversity	16, 56, 70, 74, 80 and 108
	Laser-structured Ni (nanocones, protrusions)	Periodic nanostructures, strain, high-curvature sites	Enlarged electrochemically active surface area and improved gas release	15, 16, 41 and 109–111
	Plasma/chemical etching	Controlled surface roughening and oxygen incorporation	Enhanced wettability and charge-transfer characteristics	112
Interface engineering	Ni/NiO heterostructures	Metal/oxide interfacial domains	Interfacial electronic modulation and site differentiation	55, 79, 81–83 and 94
	Ni/$Ni(OH)_2$	Hydroxylated interfacial layers	Improved surface reactivity and interfacial stability	113
	Ni/carbon interfaces	Conductive interface coupling	Improved conductivity, stability, reduced charge-transfer resistance	82
Morphology control	Nanoworms, nanowires, nanoparticles, nanocones	Size and shape engineering	High surface accessibility and efficient bubble removal	16, 22, 96 and 99–101
	3D Ni foam or hierarchical porous Ni	Porosity/3D network	Enhanced active-site accessibility and charge transport	21, 24 and 96
Defect engineering	NiO with oxygen vacancies	Vacancy-induced lattice distortion	Modified electronic structure and enhanced conductivity	101, 103, 105 and 106
	Cation vacancies, grain boundaries	Lattice non-stoichiometry	Increased density of catalytically accessible sites	50 and 84
	Ni/NiO heterostructures with engineered defects	Defect-rich interfaces	Amplified interfacial electronic effects	103 and 114
Combined strategies	Ni/NiO/C hollow composite	Combined morphology, interface, and defect engineering	Low overpotential *via* multi-parameter optimization	84
	Ni/NiO with graphene coating	Defect, interface, and conductivity control	Multifunctional activity enhancement	55, 81 and 107

Table 4 Electrochemical HER performance of representative monometallic Ni electrodes corresponding to the engineering strategies summarized in Table 3 and state-of-the-art electrodes

Strategy class	Representative system	η_{10} (mV)	Tafel slope (mV dec^{-1})	Key engineered feature	Ref.
Surface modification	Ni → $Ni(OH)_2$/NiOOH	110–140	49–120	Surface hydroxylation, $Ni^{\delta+}$ sites	16 and 56
	Ni_3N/Ni heterostructure	144	107	Interfacial electronic coupling	70
	Strain-engineered Ni/NiO (sr-NiO)	164	121	Lattice strain tuning	71
	Laser-structured Ni	120	112	High-curvature nanostructures	16
	Etched Ni-mesh	~120	68	Bubble released electrode	74
	Ni@fs-laser nanostructured Ni sheet	108	121	Dendrite-like geometry surface	40
	Fs-laser Ni nanocones	—	89	Hierarchical roughness	75
Interface engineering	Ni/NiO heterostructure	110–140	86–150	Metal/oxide junctions	50, 81 and 84
	Carbon-supported Ni/NiO	30	88	Accelerated water dissociation	82
	Ni nanoparticles on carbon	61–90	29–41	Reduced charge-transfer resistance	87 and 88
Morphology control	Ni nanoworms	109	104	Edge-rich curved surfaces	22
	Ni nanoparticles (urchin-like)	180	111	Size confinement	115
	3D Ni foam	135	99.3	High ECSA, porosity	116
	Amorphous Ni@Ni foam	45	80	Disordered active sites	117
Defect engineering	Oxygen-vacancy-rich NiO_x	120	105	Vacancy-induced conductivity	105
	Defect-rich Ni/NiO interfaces	—	63	Vacancy-assisted charge transfer	103
Combined strategies	Hollow Ni/NiO/C composite	87	91	Morphology/interface/defects engineering	84
	GO-coated Ni foam	83	55.7	Carbon defects/interface engineering	107
	Hierarchical Ni on 3D NF	80–100	55–91	Morphology/interface engineering	84 and 107
Benchmarks	Bare (unmodified) NF	217	130	Baseline substrate	118
	Pt/C	57–60	36–43	Near-zero ΔG_{H^*}	2 and 119
	Ru-doped Ni	24	31	Noble-metal d-band tuning	120
	Ni–Mo on NF/carbon cloth	15	30	Optimized ΔG_{H^*} *via* Mo incorporation	76
	Ni–Fe LDH/metallic Ni–Fe	110	77	Fe-induced electronic modulation	77
	Ni(Cu)VO_x	21	25	Interfacial/Cu assisted lattice modulation	121

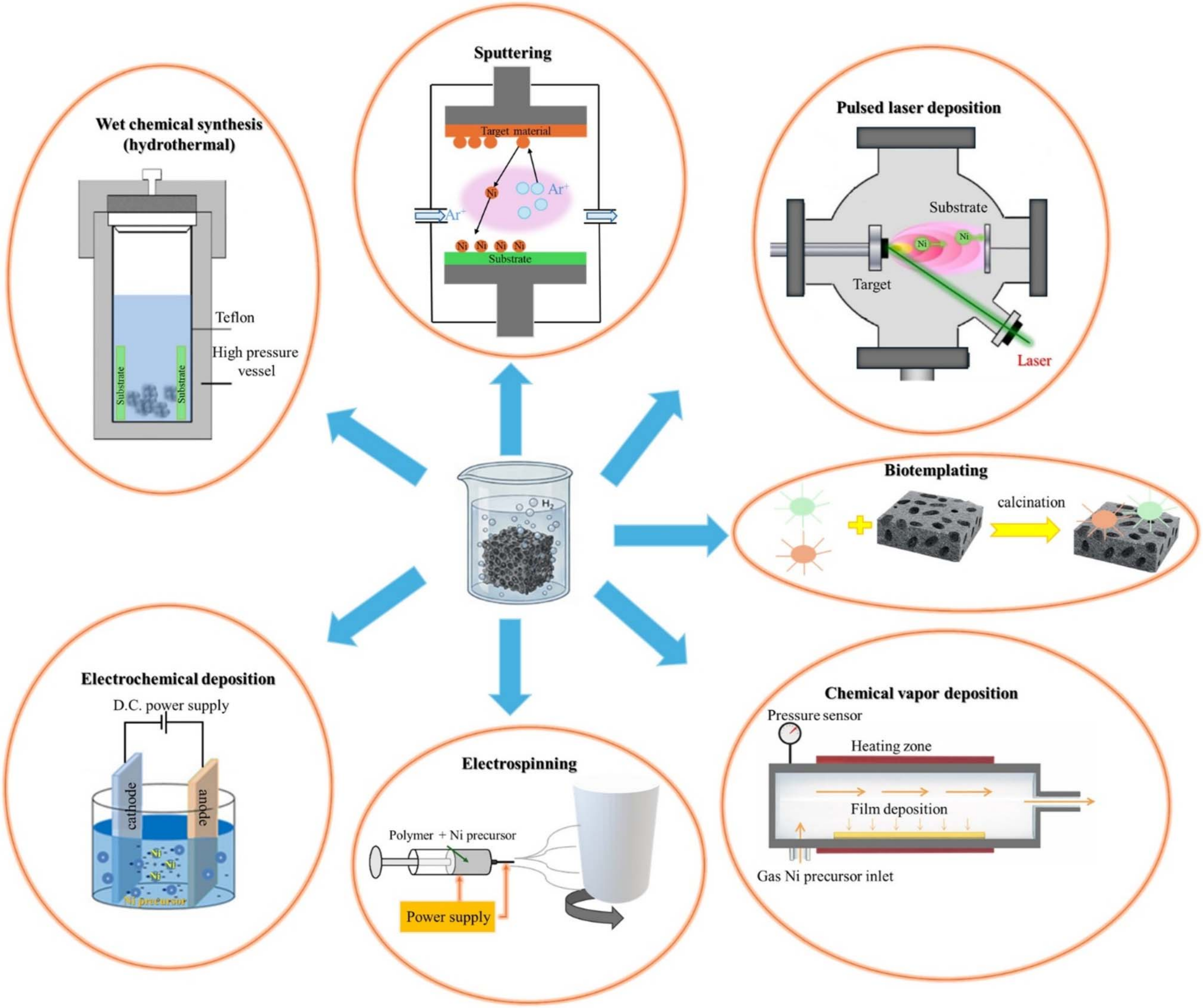

Fig. 14 Schematic illustration of representative synthesis routes for monometallic Ni-based electrodes with tailored architectures for the hydrogen evolution reaction (HER).

controllable synthesis techniques. The ability to precisely tailor surface chemistry, defect density, morphology, and interfacial structure is inherently governed by the chosen fabrication route. Accordingly, a critical understanding of available synthetic strategies – and their respective strengths and limitations – is essential for implementing the integrated catalyst architectures discussed above. In this context, the following section presents the various synthetic routes used to fabricate monometallic Ni catalysts, highlighting how each method influences structural characteristics and HER-relevant performance metrics.

6. Synthesis routes for monometallic Ni electrocatalysts

To rationalize the diverse fabrication strategies reported for monometallic Ni electrocatalysts, the synthesis routes are classified according to their dominant physical or chemical driving principles. This framework distinguishes between electron-driven growth, solution-phase chemical reactions, vapor-phase deposition processes, and template-directed structuring approaches (Fig. 14). Importantly, these categories are not mutually exclusive with respect to catalyst functionality; rather, each synthesis route enables specific combinations of surface modification, interface engineering, morphology control, and defect generation that collectively govern hydrogen evolution reaction (HER) performance. The following classification is based on the dominant physical or chemical driving force governing material formation, rather than on the resulting catalyst properties, which often overlap across synthesis routes.

6.1. Electrochemical synthesis

Electrochemical synthesis, primarily achieved *via* electrodeposition, involves the reduction of Ni^{2+} ions onto conductive substrates under an applied potential or current. This approach offers exceptional tunability over catalyst properties through

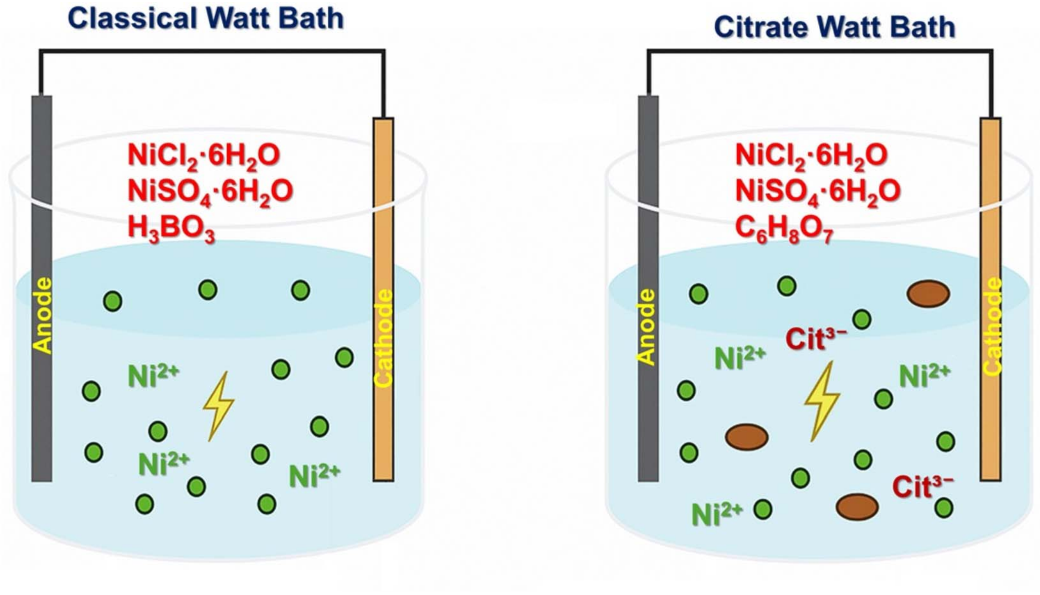

Fig. 15 Electrodeposition of Ni from a classical Watts bath and a modified citrate Watts bath.

precise control of deposition parameters, including electrolyte composition, pH, temperature, current density, and waveform (steady or pulsed).[122,123] As a result, electrodeposition enables control of grain orientation, surface roughness, porosity, and local oxidation states, making it particularly effective for tailoring the electrochemically active surface area and intrinsic hydrogen-evolution reaction (HER) kinetics.[123] Moreover, the strong coupling between deposition dynamics and substrate architecture allows electrodeposition to be readily integrated with three-dimensional supports, such as Ni foam or laser-structured Ni, facilitating hierarchical catalyst design.[40,78]

Fig. 15 schematically illustrates conventional electrodeposition in a classical Watts bath and a modified alkaline citrate bath, highlighting the fundamental differences in electrolyte chemistry governing Ni nucleation and growth. Owing to its simplicity, scalability, and low cost, electrodeposition remains one of the most widely adopted routes for fabricating monometallic Ni HER electrodes.[122]

Table 5 Key parameters and outcomes for Ni electrodeposition for HER

Parameter	Specific conditions/bath type	Observed effect on Ni deposit/HER performance	Ref.
Electrolyte	Alkaline citrate bath	Superior HER performance, lower overpotentials compared to the Watts bath	123
	Acidic Watts bath	Inferior HER performance compared to citrate bath	123
Current density	Low current density	Favors Ni(110)	125
	High current density	Favors Ni(100)	125
	50 mA cm^{-2} (citrate bath)	Achieved exchange current density 0.93 mA cm^{-2}, Tafel slope 98 mV dec^{-1}, overpotentials -210 mV (10 mA cm^{-2}) and -386 mV (100 mA cm^{-2})	123
Temperature	40 °C (citrate bath)	Best catalytic performance	123
	Decreasing temperature	Decreasing effect on peak current density of HER	125
pH	Increasing pH	Decreasing effect on peak current density of HER	125
Additives	Surfactants (ALS, DC)	Increased peak current density of HER.	125
Deposition mode	Pulsed current	Enhanced electrocatalytic activity, controlled textures and porosities	123
	Steady current	Enhanced electrochemical values, nanospheres and dendrite like morphology	40

The properties of electrodeposited Ni are highly sensitive to the electrolyte environment and electrical parameters (Table 5). Systematic studies have demonstrated that Ni electrocatalysts deposited from alkaline citrate baths consistently outperform those prepared from acidic Watts baths in HER, exhibiting lower overpotentials and improved kinetic parameters.[123] This enhanced performance is attributed not only to morphological differences but also to changes in Ni^{2+} speciation induced by citrate complexation under alkaline conditions, which alter adsorption behavior during growth and promote more favorable surface microstructures and oxidation states for HER.[123,124] Consequently, electrolyte composition plays a role as critical as electrical control in dictating atomic-level growth and catalytic functionality. The objective, therefore, is not merely to deposit Ni, but to deposit electrochemically active Ni.[36]

In modified Watts bath systems, Ni deposition proceeds through hydroxo-Ni intermediates, ultimately yielding metallic Ni *via* a multi-electron reduction pathway on conductive substrates, as described by the following reactions:[126]

$$Ni^{2+} + H_2O \rightarrow (NiOH)^+ + H^+ \tag{8}$$

$$(NiOH)^+ + e^- \rightarrow (NiOH)_{ads} \tag{9}$$

$$(NiOH)_{ads} + (NiOH)^+ + 3e^- \rightarrow 2Ni + 2OH^- \tag{10}$$

Beyond bath chemistry, substrate architecture exerts a decisive influence on catalytic performance. Porous Ni foam and laser-nanostructured Ni substrates promote high surface roughness and increased electrochemically active area, leading to reduced overpotentials, improved HER kinetics, and significantly enhanced double-layer capacitance.[40,78,116,117] Representative electrochemical metrics for electrodeposited Ni-based electrodes are summarized in Table 6, underscoring the central role of morphology-induced surface-area amplification in governing HER activity.

6.2. Wet-chemical and solvothermal synthesis

Wet-chemical synthesis methods provide a versatile platform for producing monometallic Ni catalysts with a wide diversity of morphologies that extend far beyond conventional spherical particles. Reported architectures include one-dimensional (1D) structures such as nanowires, nanotubes, nanorods, nanobelts, and nanowire chains, as well as more complex morphologies including triangular plates, hexagonal hierarchies, hollow spheres, nanosheets, and flower-like assemblies.[136,137] Among these, Ni nanowires (NiNWs) have attracted particular attention due to their high aspect ratio and intrinsic shape anisotropy, which confer enhanced electrical conductivity, directional electron transport, and magnetic responsiveness. These characteristics render NiNWs especially attractive for hydrogen evolution reaction (HER) electrocatalysis, in addition to applications in sensing, data storage, and catalysis.[136,137]

A broad range of wet-chemical synthesis techniques has been developed for fabricating nickel-based electrodes, including hydrothermal and solvothermal synthesis,[22,138–140] microwave-assisted processes,[141,142] electroless chemical reduction,[143] electrospinning-assisted routes,[144] and biologically assisted (biotemplated) synthesis.[145] These approaches allow reasonable control over particle size, crystallinity, and morphology; however, they often involve multistep procedures, specialized equipment, or stringent reaction environments that can limit scalability. For instance, electrospinning requires high-voltage operation, while biological synthesis relies on carefully controlled culture conditions. As a result, despite their structural versatility, many wet-chemical approaches face challenges when translated from laboratory-scale demonstrations to industrial HER electrode fabrication.

Table 6 Effect of synthesis method on the HER performance of Ni-based electrodes

Method	Electrode	Overpotential η_{10} (mV)	Tafel slope (mV dec^{-1})	Ref.
Electrodeposition	Electrodeposited Ni@NF	135	99.3	116
Electrodeposition	Electrodeposited amorphous Ni@NF	103	84	117
Laser nanostructuring and electrodeposition	Ni deposition on laser nanostructured Ni sheet	108	121.3	40 and 78
Electroless	Ni nanospike	327	N/A	127
Solvothermal	NiO@NF	109	103.9	22
CVD	Ni@NF	154	64	107
Electrospinning	Ni/NiO	395	152	128
Electrospun	NiO	410	258.4	129
Hydrothermal	Ni@NiO	192	106	130
Solvothermal	Urchin-Ni nanoparticles	180	111	115
Solvothermal	Hierarchical NiO	142	98	131
Biosynthesis	Ni-dinuclear	490	N/A	132
Femto second laser nanostructuring	Laser nanostructured Ni sheet	120	112	16
Femto second laser nanostructuring	Laser nanostructured Ni sheet	—	88	133
Femto second laser nanostructuring	Ni nanocones	—	89	75
Pulse laser deposition	Ni@NF	110	99	15
Physical vapor deposition	NiO_x	127	59	134
Physical vapor deposition	Ni@NF	100	88	135

Representative electrochemical HER performance metrics for chemically synthesized monometallic Ni electrodes that do not rely on noble-metal additives are summarized in Table 6. Overall, these systems exhibit moderate HER activity, with overpotentials typically exceeding those achieved *via* electrochemical deposition or interface-engineered architectures, underscoring the need for additional surface or interfacial optimization when wet-chemical routes are employed alone.

6.3. Laser-based synthesis

Laser-based fabrication and modification techniques provide a powerful, non-contact means of engineering Ni electrode surfaces with precisely controlled micro- and nanoscale features. Laser nanomachining employs high-energy, ultrafast laser pulses to induce surface structures, such as nanogrooves, pits, protrusions, and hierarchical roughness, thereby significantly increasing the electrochemically active surface area.[119,146] In addition to surface-area amplification, laser structuring enhances mass transport by facilitating electrolyte penetration and accelerating hydrogen bubble detachment, thereby improving HER kinetics.[147] The rapid localized heating and cooling associated with ultrashort laser pulses also induce crystal defects, dislocations, and residual stress fields that modify the electronic structure of surface Ni atoms and can further enhance catalytic activity.[17]

Pulsed laser deposition (PLD) represents a complementary laser-based synthesis route that enables the growth of thin Ni or Ni-based films under highly controlled vacuum or reactive atmospheres. In PLD, a high-power pulsed laser ablates a solid target, generating a plasma plume that deposits onto a substrate with precise control over film thickness, stoichiometry, and crystallinity.[148,149] This non-equilibrium growth process enables the stabilization of defect-rich, metastable, and interface-engineered Ni phases that are difficult to access *via* conventional chemical synthesis.[150] For HER applications, PLD-derived Ni films exhibit well-defined surface defects and controlled interfacial compositions, resulting in improved catalytic kinetics and durability.[16,151]

The electrochemical performance of laser-structured monometallic Ni electrodes reported in the literature is summarized in Table 6, which clearly illustrates the beneficial effects of laser-induced surface nanostructuring and interface control on HER activity.

6.4. Physical vapor deposition (PVD)

Physical vapor deposition (PVD) techniques, including sputtering and electron-beam evaporation, enable the controlled deposition of thin Ni films or nanoparticle coatings under vacuum conditions. These methods are particularly valued for their ability to produce uniform, adherent, and compositionally tunable layers, making them ideal for constructing well-defined Ni interfaces such as Ni/NiO, Ni/graphene, or dopant-modified heterostructures.[135,152,153] By precisely controlling film thickness, crystallinity, and interfacial chemistry, PVD provides a robust platform for systematic interface engineering aimed at optimizing HER kinetics.[154]

Several representative studies highlight the versatility of PVD-based Ni electrodes. For example, electron-beam evaporation of $NiCl_2$ onto ITO substrates yielded NiO_x electrodes exhibiting an overpotential $|\eta_{10}|$ of 127 mV and a relatively low Tafel slope of 59 mV dec^{-1}.[134] In another study, an eddy-current-assisted PVD setup enabled the deposition of Ni nanoparticles onto Ni foam, achieving $|\eta_{10}| \approx 100$ mV with a Tafel slope of 88 mV dec^{-1} (ref. 135) (Table 6). These results demonstrate that PVD techniques offer considerable flexibility for fabricating monometallic Ni HER electrodes with tailored surface and interfacial properties.

Importantly, laser-based methods and physical vapor deposition (PVD) enable precise control over catalyst surface structure and composition, allowing the rational tuning of active-site density, electronic conductivity, corrosion resistance, and mechanical stability. However, despite their effectiveness in engineering well-defined interfaces, their practical scalability may be constrained by relatively high fabrication costs and the need for specialized equipment. Nevertheless, these techniques remain valuable for establishing structure–property relationships and guiding the design of advanced HER electrodes that can later be translated into more cost-effective fabrication strategies.

To provide a consolidated overview of the synthesis strategies discussed in this section, Table 7 summarizes the principal fabrication routes for monometallic Ni catalysts and the structural or functional features they predominantly enable. By mapping synthesis methods to targeted catalyst properties, such as morphology control, crystallinity, interfacial composition, and defect generation, this framework highlights how the choice of fabrication route governs HER performance and

Table 7 Synthesis techniques and their influence on Ni catalyst features

Synthesis method	Targeted catalyst feature
Electrodeposition	Surface morphology, grain orientation
Hydrothermal synthesis	Crystallinity, nanostructure formation
Pulsed laser deposition (PLD)	Interface engineering, film composition
Physical vapor deposition (PVD)	Surface layer uniformity, dopant integration
Laser nanomachining	Surface roughness, active site exposure
Microwave-assisted synthesis	Nanoparticle formation, energy-efficient synthesis
Electrospinning	Template-based fiber formation, high aspect ratio
Electroless deposition	Uniform coating, simple scalability
Biosynthesis	Green synthesis of nanostructures, biological reduction

practical applicability. Collectively, these insights provide a rational basis for guiding the future design and optimization of monometallic Ni-based HER electrocatalysts.

7. Current challenges and future trends

Despite considerable advances in the development and optimization of monometallic Ni-based electrocatalysts for the hydrogen evolution reaction (HER), several critical challenges remain that hinder their widespread adoption as viable alternatives to noble-metal catalysts, such as platinum. To bridge the performance gap and unlock the full potential of Ni in water electrolysis, future research must address these limitations across multiple dimensions, including activity, kinetics, stability, structural optimization, and electrolyte adaptability. The main challenges and proposed directions are discussed below to guide research toward the development of cost-effective and highly active Ni-based electrodes for real-world industrial applications.

7.1. Bridging the intrinsic kinetic gap

Although significant progress has been made through strategies such as nanostructuring, doping, defect engineering, and surface modification, the intrinsic catalytic activity of pure Ni still lags behind that of platinum, particularly in the overpotential required to achieve high current densities. While Pt-based electrodes typically deliver 10 mA cm^{-2} at overpotentials around 40–60 mV, even optimized Ni architectures often require higher overpotential to achieve comparable current densities in alkaline media (Tables 4 and 6). The relatively sluggish water dissociation step (Volmer step) on Ni surfaces remains a bottleneck in alkaline electrolytes due to weaker OH* binding and slower H* formation, limiting the overall HER kinetics.[35] This weak interaction destabilizes the transition state for water cleavage, creating a high activation energy barrier that cannot be surmounted simply by increasing the electrochemically active surface area (ECSA). Consequently, the sluggish generation of H* protons remains the rate-determining step (RDS) for pure Ni surfaces in alkaline electrolytes.[155] To fundamentally elevate nickel's competitiveness relative to platinum, future research must shift focus from simply increasing the number of active sites to enhancing the quality of each site (intrinsic electronic properties). Three critical directions for achieving this breakthrough are suggested.

7.1.1. Crystal facet engineering. Most syntheses preferentially expose thermodynamically stable low-index Ni planes (*e.g.*, (111), (100)). However, microkinetic/DFT studies generally predict that under-coordinated Ni sites (often modeled by high-index or stepped surfaces) can reduce the activation barrier for alkaline Volmer water dissociation relative to close-packed terraces; consequently, the overall HER rate reflects the balance between water activation at defect-like motifs and H* recombination on metallic Ni domains.[156,157] These surfaces possess a high density of atomic steps, edges, and "kinks" that can serve as preferential docking sites for water molecules. Thus, future synthetic efforts should prioritize developing electrochemical pulse sequences or facet-selective capping agents that stabilize these metastable high-index surfaces during crystal growth. To this end, emerging techniques such as *operando* spectroscopy, scanning tunneling microscopy (STM), and DFT simulations can provide deeper insight into the active centers of Ni surfaces, thereby enabling rational catalyst design with maximal atomic efficiency.

7.1.2. Tuning d-band center. Instead of surface alloying, which can block active Ni sites, "strain engineering" offers a non-invasive pathway to modulate reactivity. By inducing tensile lattice strain – either through substrate lattice mismatch or rapid thermal processing – it is possible to upshift the d-band center of surface Ni atoms. This upshift strengthens interactions with the antibonding orbitals of adsorbates, thereby enhancing the binding energy of OH* intermediates without significantly compromising H* desorption.[158] Systematic studies correlating lattice strain percentage with Volmer step kinetics are a necessary next step.

7.1.3. Subsurface electronic modification. A promising yet underexplored frontier is the decoupling of surface catalytic properties from bulk composition. Rather than doping the surface directly, future strategies should explore subsurface engineering, where heteroatoms (*e.g.*, transition metals, N, B, or C) or vacancy clusters are introduced beneath the topmost Ni atomic layer.[159–161] This approach could leverage ligand and strain effects to modify the electron density at the surface Ni, facilitating water attack, while retaining a pristine metallic surface for efficient hydrogen recombination. This "subsurface-doping" strategy effectively mimics the electronic behavior of noble metals while maintaining the chemical identity of a pure Ni surface.

Looking ahead, the integration of data-driven design frameworks that combine Density Functional Theory (DFT), Machine Learning (ML), and high-throughput experimentation offers a transformative pathway for navigating the complex parameter space of catalyst morphology, defect density, and interfacial electronic structure. By moving beyond traditional trial-and-error, these approaches can accelerate the identification of optimal structure–property relationships.[162,163] Crucially, the utility of these computational tools relies on their coupling with experimentally verifiable descriptors and standardized performance metrics to ensure predictive reliability and reproducibility.

7.2. From lab-scale durability to industrial viability

While Ni demonstrates favorable corrosion resistance in alkaline media, its long-term stability at industrially relevant current densities (≥500 mA cm^{-2}) remains a critical bottleneck. Under these vigorous conditions, the catalyst is subjected to severe stress driven by rapid gas bubble evolution, which can fracture delicate nanostructures and cause delamination, failure modes that are rarely captured during short-term, low-current laboratory testing.[164] Furthermore, a significant "scalability gap" persists; many high-performance architectures synthesized *via* batch methods (*e.g.*, hydrothermal autoclaves) lack the uniformity and mechanical robustness required for large-area deployment, effectively preventing their translation from laboratory prototypes to industrial stacks.

To bridge this gap, future research must pivot from static "activity" evaluation to rigorous Accelerated Stress Tests (ASTs) and manufacturing-oriented design. Standard testing protocols should move beyond constant-current operation to incorporate dynamic load cycling that simulates the intermittency of renewable energy inputs (*e.g.*, solar/wind) to reveal degradation mechanisms that are hidden in static tests. Concurrently, synthesis strategies must transition from batch processing to continuous Roll-to-Roll (R2R) compatible techniques, such as high-speed electrodeposition or continuous hydrothermal synthesis. Integrating these scalable methods with surface engineering and regeneration approaches that promote rapid bubble release will be essential to mitigate mechanical stress and ensure the integrity of nanostructured Ni catalysts at the industrial scale.

7.2.1. Electrolyte-dependent behavior and stability. Electrolyte composition remains a critical determinant of catalytic efficacy. While monometallic Ni exhibits optimal performance in alkaline media, its activity and stability are severely compromised in neutral and acidic environments. In acidic conditions, thermodynamic instability leads to rapid corrosion, while in neutral media, sluggish water dissociation kinetics hinder reaction rates. These limitations currently restrict the integration of Ni-based catalysts into Proton Exchange Membrane (PEM) electrolyzers and direct seawater splitting systems.[165] Overcoming these barriers requires advanced mitigation strategies, including surface functionalization with proton-conducting or anti-corrosion layers, the engineering of hybrid electrode architectures, and the design of bifunctional surfaces that effectively decouple the water dissociation step from hydrogen adsorption.[166,167]

7.2.2. System-level considerations. Finally, bridging the gap between laboratory innovation and industrial deployment necessitates a shift toward system-level evaluation. Future research must prioritize assessing electrode durability under fluctuating power inputs (representative of intermittent renewable energy sources), tolerance to electrolyte impurities (*e.g.*, chloride-induced corrosion in seawater), and overall life-cycle sustainability.[168,169] Addressing these practical constraints, alongside fundamental catalytic optimization, is essential for advancing monometallic Ni electrodes from promising laboratory materials to viable components for large-scale green hydrogen production.

8. Conclusion

Monometallic nickel has solidified its position as a compelling electrocatalyst platform for the hydrogen evolution reaction (HER), effectively balancing earth abundance, cost efficiency, and intrinsic electrochemical stability in alkaline environments. As demonstrated throughout this review, advances in surface modification, interface engineering, defect engineering, and morphology control have collectively transformed Ni from a baseline catalyst into a highly competitive HER electrode. Rational tuning of surface oxidation states, construction of Ni/NiO and Ni/Ni(OH)$_2$ heterointerfaces, and introduction of vacancy defects effectively modulate the hydrogen adsorption free energy ($\Delta G_{\mathrm{H}*}$), accelerate water dissociation, and maximize active-site density.

Notably, a growing body of experimental and computational evidence indicates that the catalytically active state of Ni is not a static metallic surface, but a dynamically reconstructed interface comprising metallic Ni coupled with hydroxylated or oxide-derived domains. These self-adaptive interfaces regulate the surface electronic structure and active-site accessibility, thereby enhancing HER kinetics under operational conditions. Consequently, numerous monometallic Ni architectures, ranging from electrodeposited foams to laser-nanostructured sheets, now exhibit kinetics that rival those of complex alloys.

Beyond intrinsic activity, Ni offers decisive advantages for practical deployment, including compatibility with commercial alkaline stacks, mechanical robustness at elevated current densities, and scalability through mature fabrication routes such as electrodeposition, thermal processing, and laser nanomachining. While challenges remain, particularly in extending performance to acidic or neutral media and ensuring durability under fluctuating power loads, the progress summarized here establishes monometallic Ni as far more than a model system. Instead, it represents a technologically viable and strategically important cathode material for next-generation alkaline hydrogen production.

In summary, this review elucidates the critical design principles required to elevate monometallic nickel to state-of-the-art performance, challenging the traditional assumption that noble metals or complex alloys are prerequisites for efficient HER. By decoupling the specific contributions of morphology, defect engineering, and dynamic surface reconstruction, the analysis presented here offers a unified blueprint for rational catalyst design. These insights demonstrate that the path forward lies not in empirical trial-and-error, but in the deliberate coupling of *operando*-verified mechanistic understanding with industrially scalable synthesis. Realizing this combination will be essential to cement nickel's role as a cornerstone material in the global transition toward sustainable hydrogen technologies.

Conflicts of interest

There are no conflicts to declare.

Data availability

No primary research results, software, or code have been included, and no new data were generated or analyzed as part of this review.

Acknowledgements

The publication of the article in OA mode was financially supported by HEAL-Link.

References

1 X. Peng, *et al.*, Recent advance and prospectives of electrocatalysts based on transition metal selenides for efficient water splitting, *Nano Energy*, 2020, **78**, 105234.

2 A. Kazemi, F. Manteghi and Z. Tehrani, Metal Electrocatalysts for Hydrogen Production in Water Splitting, *ACS Omega*, 2024, **9**(7), 7310–7335.

3 V. Vij, *et al.*, Nickel-Based Electrocatalysts for Energy-Related Applications: Oxygen Reduction, Oxygen Evolution, and Hydrogen Evolution Reactions, *ACS Catal.*, 2017, **7**, 7196–7225.

4 D. J. Jovan and G. Dolanc, Can Green Hydrogen Production Be Economically Viable under Current Market Conditions, *Energies*, 2020, **13**, 6599.

5 L. Xiong, Y. Qiu, X. Peng, Z. Liu and P. K. Chu, Electronic structural engineering of transition metal-based electrocatalysts for the hydrogen evolution reaction, *Nano Energy*, 2022, **104**, 107882.

6 G. Zhao, K. Rui, S. X. Dou and W. Sun, Heterostructures for Electrochemical Hydrogen Evolution Reaction: A Review, *Adv. Funct. Mater.*, 2018, **28**(43), 1803291.

7 X. Zou and Y. Zhang, Noble metal-free hydrogen evolution catalysts for water splitting, *Chem. Soc. Rev.*, 2015, **44**, 5148–5180.

8 H. Li, J. Wu, M. Li and Y. Wang, Recent Advances in Vanadium-Based Electrocatalysts for Hydrogen and Oxygen Evolution Reactions: A Review, *Catalysts*, 2024, **14**, 368.

9 F. Safizadeh, E. Ghali and G. Houlachi, Electrocatalysis developments for hydrogen evolution reaction in alkaline solutions – A Review, *Int. J. Hydrogen Energy*, 2015, **40**, 256–274.

10 F. Farzinpour, A. A. Ensafi, K. Zarean Mousaabadi and B. Rezaei, Synthesis and study of electrochemical properties of Ni-Co-V@PrGO to enhance hydrogen evolution reaction, *Int. J. Hydrogen Energy*, 2023, **48**, 21249–21258.

11 S. Abolghasemi Fakhri, H. Ashassi-Sorkhabi, E. Asghari, M. T. Taghizadeh and H. Javan, Edge-halogenated graphene nanosheets as an efficient metal-free electrocatalyst for hydrogen evolution reaction, *Int. J. Hydrogen Energy*, 2022, **47**, 15731–15741.

12 H. Zhao, *et al.*, Fabrication of CoM (M = Ni, Cu) alloys modified carbon electrocatalysts by pyrolysis of dual-metal-site metal-organic frameworks for efficient dye-sensitized solar cells, *J. Alloys Compd.*, 2024, **1006**, 176278.

13 N. H. Teleb, *et al.*, First-principles study of doped hexagonal silicon carbide nanotubes as bifunctional water splitting electrocatalysts, *Int. J. Hydrogen Energy*, 2025, **150**, 150084.

14 W.-F. Chen, J. T. Muckerman and E. Fujita, Recent developments in transition metal carbides and nitrides as hydrogen evolution electrocatalysts, *Chem. Commun.*, 2013, **49**, 8896.

15 I. A. Poimenidis, *et al.*, Ni foam electrodes decorated with Ni nanoparticles via pulsed laser deposition for efficient hydrogen evolution reaction, *Mater. Sci. Eng., B*, 2024, **299**, 116922.

16 I. A. Poimenidis, *et al.*, Enhanced hydrogen production through alkaline electrolysis using laser-nanostructured nickel electrodes, *Int. J. Hydrogen Energy*, 2021, **46**, 37162–37173.

17 S. Wang, *et al.*, Controllable synthesis of nickel nanowires and its application in high sensitivity, stretchable strain sensor for body motion sensing, *J. Mater. Chem. C*, 2018, **6**, 4737–4745.

18 T. Wasiak, L. Przypis, K. Z. Walczak and D. Janas, Nickel Nanowires: Synthesis, Characterization and Application as Effective Catalysts for the Reduction of Nitroarenes, *Catalysts*, 2018, **8**, 566.

19 O. A. Logutenko, A. I. Titkov, A. M. Vorob'yov, Y. M. Yukhin and N. Z. Lyakhov, Characterization and Growth Mechanism of Nickel Nanowires Resulting from Reduction of Nickel Formate in Polyol Medium, *J. Nanomater.*, 2016, **2016**, 1–9.

20 A. Shahzad, *et al.*, Synthesis of nickel nanowires (Ni-NWs) as high ferromagnetic material by electrodeposition technique, *Heliyon*, 2023, **9**, e12576.

21 I. A. Poimenidis, M. Lykaki, P. A. Loukakos and M. Konsolakis, Ultra-high supercapacitor performance of NiSRu@NiO nanocomposites on nickel foam electrodes, *J. Energy Storage*, 2024, **83**, 110679.

22 I. A. Poimenidis, M. Lykaki, S. Moustaizis, P. Loukakos and M. Konsolakis, One-step solvothermal growth of NiO nanoparticles on nickel foam as a highly efficient electrocatalyst for hydrogen evolution reaction, *Mater. Chem. Phys.*, 2023, **305**, 128007.

23 N. I. Hafiz, M. A. Islam and S. Saha, Characterization of synthesized nickel foam using ammonium hydrogen carbonate as space holder, *Results Eng.*, 2024, **24**, 103634.

24 M. P. Browne, *et al.*, Improving the performance of porous nickel foam for water oxidation using hydrothermally prepared Ni and Fe metal oxides, *Sustainable Energy Fuels*, 2017, **1**, 207–216.

25 X. Zhang, Y. Guo and C. Wang, Multi-interface engineering of nickel-based electrocatalysts for alkaline hydrogen evolution reaction, *Energy Mater.*, 2024, **4**(4), 115.

26 N. A. Khan, *et al.*, Recent Development of Nanostructured Nickel Metal-Based Electrocatalysts for Hydrogen Evolution Reaction: A Review, *Top. Catal.*, 2023, **66**, 149–181.

27 F. Chen, *et al.*, Monometallic interphase synergistic Ni-based catalysts prepared by facile magnetron sputtering for efficient alkaline hydrogen evolution, *J. Alloys Compd.*, 2024, **976**, 173103.

28 L. Huo, *et al.*, Applications of Nickel-Based Electrocatalysts for Hydrogen Evolution Reaction, *Adv. Energy Sustainability Res.*, 2022, **3**, 2100189.

29 W. Lu, *et al.*, Defect engineering of electrode materials towards superior reaction kinetics for high-performance supercapacitors, *J. Mater. Chem. A*, 2022, **10**, 15267–15296.

30 I. M. Perović, S. D. Mitrović, S. M. Brković and I. A. Pašti, Advances in Nickel-Based Catalysts for Alkaline Water

Electrolysis: Comprehensive Review of Current Research Direction for HER and OER Applications, *Chem. Rec.*, 2025, **25**, e202500049.

31 X. Ding, *et al.*, Dynamic restructuring of nickel sulfides for electrocatalytic hydrogen evolution reaction, *Nat. Commun.*, 2024, **15**, 5336.

32 M. Gong, D.-Y. Wang, C.-C. Chen, B.-J. Hwang and H. Dai, A mini review on nickel-based electrocatalysts for alkaline hydrogen evolution reaction, *Nano Res.*, 2016, **9**, 28–46.

33 M. López, K. S. Exner, F. Viñes and F. Illas, Theoretical study of the mechanism of the hydrogen evolution reaction on the V_2C MXene: Thermodynamic and kinetic aspects, *J. Catal.*, 2023, **421**, 252–263.

34 E. Santos, P. Hindelang, P. Quaino and W. Schmickler, A model for the Heyrovsky reaction as the second step in hydrogen evolution, *Phys. Chem. Chem. Phys.*, 2011, **13**, 6992.

35 M. Lao, *et al.*, From fundamentals and theories to heterostructured electrocatalyst design: An in-depth understanding of alkaline hydrogen evolution reaction, *Nano Energy*, 2022, **98**, 107231.

36 Z. Angeles-Olvera, *et al.*, Nickel-Based Electrocatalysts for Water Electrolysis, *Energies*, 2022, **15**, 1609.

37 C. Wan, *et al.*, Unraveling and Resolving the Inconsistencies in Tafel Analysis for Hydrogen Evolution Reactions, *ACS Cent. Sci.*, 2024, **10**, 658–665.

38 M. Kibria, Electrochemical studies of a nickel electrode for the hydrogen evolution reaction, *Int. J. Hydrogen Energy*, 1995, **20**, 435–440.

39 S. Wang, A. Lu and C.-J. Zhong, Hydrogen production from water electrolysis: role of catalysts, *Nano Convergence*, 2021, **8**, 4.

40 I. A. Poimenidis, *et al.*, Electrodeposited laser – nanostructured electrodes for increased hydrogen production, *Int. J. Hydrogen Energy*, 2022, **47**, 9527–9536.

41 I. Poimenidis, *et al.*, in *Laser-Nanostructured Substrates for Enhanced Hydrogen Evolution Reaction*, ed. A. V. Kabashin, M. Farsari and M. Mahjouri-Samani, SPIE, 2024, p. 1, DOI: 10.1117/12.3003827.

42 B. Abderezzak, Charge Transfer Phenomena, in *Introduction to Transfer Phenomena in PEM Fuel Cell*, Elsevier, 2018, pp. 53–83, DOI: 10.1016/B978-1-78548-291-5.50002-0.

43 H. Cruz-Martínez, *et al.*, Current progress of Pt-based ORR electrocatalysts for PEMFCs: An integrated view combining theory and experiment, *Mater. Today Phys.*, 2021, **19**, 100406.

44 J. Ryl, J. Wysocka, P. Slepski and K. Darowicki, Instantaneous impedance monitoring of synergistic effect between cavitation erosion and corrosion processes, *Electrochim. Acta*, 2016, **203**, 388–395.

45 P. A. Kempler and A. C. Nielander, Reliable reporting of Faradaic efficiencies for electrocatalysis research, *Nat. Commun.*, 2023, **14**, 1158.

46 L. Gao, *et al.*, A nickel nanocatalyst within a h-BN shell for enhanced hydrogen oxidation reactions, *Chem. Sci.*, 2017, **8**, 5728–5734.

47 C. Traisnel, A. Metsue, A. Oudriss, J. Bouhattate and X. Feaugas, Hydrogen solubility and diffusivity near surface of nickel single crystals: Some implications of elastic energy, *Comput. Mater. Sci.*, 2021, **188**, 110136.

48 S. Tsatsos and G. Kyriakou, Copper Growth on a Stepped Nickel Surface: Electronic and Geometric Effects on CO Reactivity, *J. Phys. Chem. C*, 2023, **127**, 6337–6346.

49 L. Peng, *et al.*, Chimney effect of the interface in metal oxide/metal composite catalysts on the hydrogen evolution reaction, *Appl. Catal., B*, 2019, **245**, 122–129.

50 F. Zhou and G. Tao, Structure Sensitivity in Hydrogen Adsorption on Ni/NiO Interfaces for the Hydrogen Evolution Reaction, *J. Phys. Chem. C*, 2023, **127**, 23180–23188.

51 Y. Cheng, *et al.*, Accelerated water dissociation kinetics by nickel-nickelous hydroxide epitaxial interfaces for superior alkaline hydrogen generation, *J. Colloid Interface Sci.*, 2025, **679**, 600–608.

52 A. Y. Faid, A. O. Barnett, F. Seland and S. Sunde, Ni/NiO nanosheets for alkaline hydrogen evolution reaction: In situ electrochemical-Raman study, *Electrochim. Acta*, 2020, **361**, 137040.

53 M. Arya, *et al.*, DFT studies of hydrocarbon combustion on metal surfaces, *J. Mol. Model.*, 2018, **24**, 47.

54 A. Mohsenzadeh, T. Richards and K. Bolton, DFT study of the water gas shift reaction on Ni(111), Ni(100) and Ni(110) surfaces, *Surf. Sci.*, 2016, **644**, 53–63.

55 R. M. S. Yoo, D. Yesudoss, D. Johnson and A. Djire, A Review on the Application of In-Situ Raman Spectroelectrochemistry to Understand the Mechanisms of Hydrogen Evolution Reaction, *ACS Catal.*, 2023, **13**, 10570–10601.

56 W. Lai, *et al.*, In situ Raman spectroscopic study towards the growth and excellent HER catalysis of $Ni/Ni(OH)_2$ heterostructure, *Int. J. Hydrogen Energy*, 2021, **46**, 26861–26872.

57 Q. Ma, *et al.*, Identifying the electrocatalytic sites of nickel disulfide in alkaline hydrogen evolution reaction, *Nano Energy*, 2017, **41**, 148–153.

58 A. Suzuki, *et al.*, *In Situ* Shell-Isolated Nanoparticle-Enhanced Raman Spectroscopy Study of Nickel Surface Oxides Reveals Previously Unseen Surface Chemical Dynamics, *ACS Electrochem.*, 2025, **1**, 873–885.

59 C. W. Thurner, *et al.*, New Insights into the Hydrogen Evolution Mechanism near the Ni/YSZ Triple Phase Boundary during Steam Electrolysis: A Patterned Model Electrode Study, *ACS Electrochem.*, 2025, **1**, 315–327.

60 C. Liu, *et al.*, Manipulating d-Band Center of Nickel by Single-Iodine-Atom Strategy for Boosted Alkaline Hydrogen Evolution Reaction, *J. Am. Chem. Soc.*, 2024, **146**, 26844–26854.

61 J. Zhang, *et al.*, Atomic mechanisms of hexagonal close-packed Ni nanocrystallization revealed by in situ liquid cell transmission electron microscopy, *Nano Res.*, 2022, **15**, 6772–6778.

62 J. Matsuda, *In situ* TEM studies on hydrogen-related issues: hydrogen storage, hydrogen embrittlement, fuel cells and electrolysis, *Microscopy*, 2024, **73**, 196–207.

63 K. M. Kamal, *et al.*, Precise design and construction of NiO-Ni heterostructures for active hydrogen evolution photocatalysis, *Appl. Catal. O: Open*, 2024, **194**, 206997.

64 J. Sun, S. Xu, W. Gao and G. Zhao, Engineering the Local Electronic Configuration of Diatomic Iron–Nickel Site for Enhanced Nitrate and Ammonia Co-Electrolysis Activity, *Small*, 2025, **21**, 2409239.

65 Z. Zhou, *et al.*, Unlocking Catalytic Potential in Electrochemical Energy Transformations by Strain Engineering, *ChemistryEurope*, 2025, e202500285, DOI: 10.1002/ceur.202500285.

66 C. K. W. Lee, Y. Pan, R. Yang, M. Kim and M. G. Li, Laser-Induced Transfer of Functional Materials, *Top. Curr. Chem.*, 2023, **381**, 18.

67 R. W. Cross and N. Y. Dzade, First-Principles Mechanistic Insights into the Hydrogen Evolution Reaction on Ni_2P Electrocatalyst in Alkaline Medium, *Catalysts*, 2020, **10**, 307.

68 D. Wang, Q. Li, C. Han, Z. Xing and X. Yang, When NiO@Ni Meets WS_2 Nanosheet Array: A Highly Efficient and Ultrastable Electrocatalyst for Overall Water Splitting, *ACS Cent. Sci.*, 2018, **4**, 112–119.

69 P. Prabhu and J.-M. Lee, Influencing electrocatalytic processes through topographically disordered atomic sites, *Chem Catal.*, 2023, **3**, 100621.

70 L. Xiong, *et al.*, Metallic Ni_3N/Ni heterostructure for efficient hydrogen evolution reaction, *Int. J. Hydrogen Energy*, 2024, **59**, 400–407.

71 X. Yi, X. He, F. Yin, G. Li and Z. Li, Surface strain engineered Ni-NiO for boosting hydrogen evolution reaction in alkaline media, *Electrochim. Acta*, 2021, **391**, 138985.

72 T. Meng, *et al.*, Electrochemically induced in-situ surface self-reconstruction on Ni, Fe, Zn ternary-metal hydroxides towards the oxygen-evolution performance, *Chem. Eng. J.*, 2021, **410**, 128331.

73 S. Kumaravel, *et al.*, *In situ* electrochemical transformation of Ni^{2+} to NiOOH as an effective electrode for water oxidation reaction, *Dalton Trans.*, 2022, **51**, 17454–17465.

74 J. Ma, *et al.*, Ni electrodes with 3D-ordered surface structures for boosting bubble releasing toward high current density alkaline water splitting, *Ultrason. Sonochem.*, 2023, **96**, 106398.

75 T. Rauscher, *et al.*, Femtosecond-laser structuring of Ni electrodes for highly active hydrogen evolution, *Electrochim. Acta*, 2017, **247**, 1130–1139.

76 J. Zhang, *et al.*, Efficient hydrogen production on $MoNi_4$ electrocatalysts with fast water dissociation kinetics, *Nat. Commun.*, 2017, **8**, 15437.

77 P. Xiong, *et al.*, Interface Modulation of Two-Dimensional Superlattices for Efficient Overall Water Splitting, *Nano Lett.*, 2019, **19**, 4518–4526.

78 I. A. Poimenidis, *et al.*, Electrodeposition of Ni particles on laser nanostructured electrodes for enhanced hydrogen evolution reaction, *Mater. Today: Proc.*, 2022, **67**(Part 7), 953–958.

79 S. Lalwani, M. AlNahyan, A. Al Zaabi, F. AlMarzooqi and A. Qurashi, Advances in Interfacial Engineering and Their Role in Heterostructure Formation for HER Applications in Wider pH, *ACS Appl. Energy Mater.*, 2022, **5**, 14571–14592.

80 D. Neumüller, *et al.*, Hydrogen Evolution Reaction on Ultra-Smooth Sputtered Nanocrystalline Ni Thin Films in Alkaline Media—From Intrinsic Activity to the Effects of Surface Oxidation, *Nanomaterials*, 2023, **13**, 2085.

81 J. Wang, *et al.*, Ni/NiO heterostructures encapsulated in oxygen-doped graphene as multifunctional electrocatalysts for the HER, UOR and HMF oxidation reaction, *Catal. Sci. Technol.*, 2021, **11**, 2480–2490.

82 C. Li, *et al.*, Accelerating water dissociation at carbon supported nanoscale Ni/NiO heterojunction electrocatalysts for high-efficiency alkaline hydrogen evolution, *Nano Res.*, 2023, **16**, 4742–4750.

83 Y. Liu, Z. Liu, L. Jia, D. Gao and Z. Tang, Interface engineering of Ni/NiO hierarchical heterojunction for oxygen evolution reaction: A combined experimental and theoretical study, *Appl. Surf. Sci.*, 2022, **606**, 154897.

84 H. H. Do, *et al.*, Hollow Ni/NiO/C composite derived from metal-organic frameworks as a high-efficiency electrocatalyst for the hydrogen evolution reaction, *Nano Convergence*, 2023, **10**, 6.

85 Y.-F. Xing, *et al.*, Bifunctional mechanism of hydrogen oxidation reaction on atomic level tailored-Ru@Pt core-shell nanoparticles with tunable Pt layers, *J. Electroanal. Chem.*, 2020, **872**, 114348.

86 I. Poimenidis, E. Skliri, E. Kourmouli, V. Binas and M. Konsolakis, Tailoring nickel foam-based electrocatalysts via oxidation-reduction pretreatment and Ni deposition for enhanced oxygen evolution reaction in alkaline media, *J. Power Sources*, 2026, **676**, 239802.

87 S. Abolghasemi Fakhri, H. Ashassi-Sorkhabi, E. Asghari and H. Javan, A novel electrodeposited nanocatalyst of nickel nanoparticles and reduced graphene oxide doped with halogens for hydrogen evolution reaction, *Sci. Rep.*, 2025, **15**, 13567.

88 H. Wang, J. Xu, J. Xie, C. Wang and P. Bai, Hydrogen evolution performance of Ni loading on the carbon-based catalysts, *Mater. Chem. Phys.*, 2021, **272**, 125049.

89 A. Goyal, S. Louisia, P. Moerland and M. T. M. Koper, Cooperative Effect of Cations and Catalyst Structure in Tuning Alkaline Hydrogen Evolution on Pt Electrodes, *J. Am. Chem. Soc.*, 2024, **146**, 7305–7312.

90 C. M. Schott, *et al.*, How to Assess and Predict Electrical Double Layer Properties. Implications for Electrocatalysis, *Chem. Rev.*, 2024, **124**, 12391–12462.

91 Q. Zhang, P. Sun, H. Li and Z. Duan, Synergistic cation-facet effects boost alkaline hydrogen evolution kinetics on stepped Pt surfaces, *Commun. Chem.*, 2026, **9**, 113.

92 J. A. D. del Rosario, G. Li, M. F. M. Labata, J. D. Ocon and P.-Y. A. Chuang, Unravelling the roles of alkali-metal cations for the enhanced oxygen evolution reaction in alkaline media, *Appl. Catal., B*, 2021, **288**, 119981.

93 Š. Trafela, J. Zavašnik, S. Šturm and K. Ž. Rožman, Formation of a $Ni(OH)_2$/NiOOH active redox couple on

nickel nanowires for formaldehyde detection in alkaline media, *Electrochim. Acta*, 2019, **309**, 346–353.

94 Z. Du, S. Zhang, Y. Xing and X. Wu, Nanocone-arrays supported tin-based anode materials for lithium-ion battery, *J. Power Sources*, 2011, **196**, 9780–9785.

95 N. Kaur, E. Comini, N. Poli, D. Zappa and G. Sberveglieri, Nickel Oxide Nanowires Growth by VLS Technique for Gas Sensing Application, *Procedia Eng.*, 2015, **120**, 760–763.

96 A. M. El-Khatib, M. S. Badawi, G. D. Roston, R. M. Moussa and M. M. Mohamed, Structural and Magnetic Properties of Nickel Nanoparticles Prepared by Arc Discharge Method Using an Ultrasonic Nebulizer, *J. Cluster Sci.*, 2018, **29**, 1321–1327.

97 A. Baghban, S. Habibzadeh and F. Z. Ashtiani, New insights into the hydrogen evolution reaction using Ni-ZIF8/67-derived electrocatalysts, *Sci. Rep.*, 2023, **13**, 8359.

98 D. Degerman, *et al.*, State of the Surface During CO Hydrogenation over Ni(111) and Ni(211) Probed by Operando X-ray Photoelectron Spectroscopy, *J. Phys. Chem. C*, 2023, **127**, 4021–4032.

99 S. Rana, N. Masli, D. S. Monder and A. Chatterjee, Hydriding pathway for Ni nanoparticles: Computational characterization provides insights into the nanoparticle size and facet effect on layer-by-layer subsurface hydride formation, *Comput. Mater. Sci.*, 2022, **210**, 111482.

100 S. Piskunov, G. Zvejnieks, Y. F. Zhukovskii and S. Bellucci, Atomic and electronic structure of both perfect and nanostructured Ni(111) surfaces: First-principles calculations, *Thin Solid Films*, 2011, **519**, 3745–3751.

101 N. M. Rasi, S. Ponnurangam and N. Mahinpey, First-principles investigations into the effect of oxygen vacancies on the enhanced reactivity of NiO via Bader charge and density of states analysis, *Catal. Today*, 2023, **407**, 172–181.

102 Manju, *et al.*, Oxygen vacancies induced photoluminescence in $SrZnO_2$ nanophosphors probed by theoretical and experimental analysis, *Sci. Rep.*, 2020, **10**, 17364.

103 K. Zhang, *et al.*, Interface engineering of Ni/NiO heterostructures with abundant catalytic active sites for enhanced methanol oxidation electrocatalysis, *J. Colloid Interface Sci.*, 2023, **630**, 570–579.

104 D. Yuk, *et al.*, Improving the Optoelectrical Properties of a Nickel Oxide Hole Transport Layer by Hydrogen Peroxide Treatment for Efficient Organic Solar Cells, *ACS Appl. Energy Mater.*, 2024, **7**, 4558–4564.

105 F. Foroughi, *et al.*, In Situ Sonoactivation of Polycrystalline Ni for the Hydrogen Evolution Reaction in Alkaline Media, *ACS Appl. Energy Mater.*, 2023, **6**, 4520–4529.

106 P. Gao, *et al.*, The Role of Cation Vacancies in Electrode Materials for Enhanced Electrochemical Energy Storage: Synthesis, Advanced Characterization, and Fundamentals, *Adv. Energy Mater.*, 2020, **10**(14), 1903780.

107 S. Sarawutanukul, N. Phattharasupakun and M. Sawangphruk, 3D CVD graphene oxide-coated Ni foam as carbo- and electro-catalyst towards hydrogen evolution reaction in acidic solution: In situ electrochemical gas chromatography, *Carbon*, 2019, **151**, 109–119.

108 J. Zhang, T. Zhang and S. Feng, Mechanism investigation of α-Ni(OH)$_2$ electrodeposition from a $NiCl_2$ solution, *Int. J. Hydrogen Energy*, 2021, **46**, 41–49.

109 I. A. Poimenidis, P. A. Loukakos and M. Konsolakis, NiO nanolayer electrodeposited with Cobalt and Phosphide as a novel supercapacitor with high areal capacitance, *J. Phys. Chem. Solids*, 2025, **196**, 112365.

110 L. Ji, C. Lv, Z. Chen, Z. Huang and C. Zhang, Nickel-Based (Photo)Electrocatalysts for Hydrogen Production, *Adv. Mater.*, 2018, **30**, 1705653.

111 R. A. Marquez, *et al.*, Insights into catalyst degradation during alkaline water electrolysis under variable operation, *Energy Environ. Sci.*, 2025, **18**, 7170–7187.

112 B. Narayanan, V. D. M. H., K. L. and S. Gurusamy, Plasma-Sprayed Nickel-Based Electrocatalysts with Molybdenum and Chromium Doping for Efficient Hydrogen and Oxygen Evolution Reactions, *Energy Fuels*, 2025, **39**, 20609–20620.

113 W. Zhong, *et al.*, Interfacial electron rearrangement: Ni activated Ni(OH)$_2$ for efficient hydrogen evolution, *J. Energy Chem.*, 2021, **61**, 236–242.

114 J. Wang, *et al.*, Dominating Role of Ni^0 on the Interface of Ni/NiO for Enhanced Hydrogen Evolution Reaction, *ACS Appl. Mater. Interfaces*, 2017, **9**, 7139–7147.

115 S. A. Abbas, M. I. Iqbal, S.-H. Kim and K.-D. Jung, Catalytic Activity of Urchin-like Ni nanoparticles Prepared by Solvothermal Method for Hydrogen Evolution Reaction in Alkaline Solution, *Electrochim. Acta*, 2017, **227**, 382–390.

116 I. A. Poimenidis, *et al.*, Electrodeposited Ni foam electrodes for increased hydrogen production in alkaline electrolysis, *Fuel*, 2023, **342**, 127798.

117 C. Miao, *et al.*, Facile Electrodeposition of Amorphous Nickel/Nickel Sulfide Composite Films for High-Efficiency Hydrogen Evolution Reaction, *ACS Appl. Energy Mater.*, 2021, **4**, 927–933.

118 X. Hu, X. Tian, Y.-W. Lin and Z. Wang, Nickel foam and stainless steel mesh as electrocatalysts for hydrogen evolution reaction, oxygen evolution reaction and overall water splitting in alkaline media, *RSC Adv.*, 2019, **9**, 31563–31571.

119 M. Nie, *et al.*, Preparation of PtAuFe/C composite catalyst and performance for hydrogen evolution reaction, *Electrochem. Commun.*, 2020, **116**, 106765.

120 J. Su, *et al.*, Ruthenium-cobalt nanoalloys encapsulated in nitrogen-doped graphene as active electrocatalysts for producing hydrogen in alkaline media, *Nat. Commun.*, 2017, **8**, 14969.

121 Y. Li, *et al.*, Implanting Ni-O-VOx sites into Cu-doped Ni for low-overpotential alkaline hydrogen evolution, *Nat. Commun.*, 2020, **11**, 2720.

122 S. Zhang, X. Zhang, Y. Rui, R. Wang and X. Li, Recent advances in non-precious metal electrocatalysts for pH-universal hydrogen evolution reaction, *Green Energy Environ.*, 2021, **6**, 458–478.

123 R. Bojîncă, R. Muntean, R. Crişan and A. Kellenberger, Nickel Electrocatalysts Obtained by Pulsed Current Electrodeposition from Watts and Citrate Baths for Enhanced Hydrogen Evolution Reaction in Alkaline Media, *Materials*, 2025, **18**, 2775.

124 T. Doi, K. Mizumoto, M. Aonuma and S. Tanaka, Properties of the Film from Nickel Electroplating Bath Using Citric Acid, *J. Surf. Finish. Soc. Jpn.*, 2002, **53**, 335–340.

125 E. S. Güler, E. Konca and İ. Karakaya, Effect of Electrodeposition Parameters on the Current Density of Hydrogen Evolution Reaction in Ni and Ni-MoS_2 Composite Coatings, *Int. J. Electrochem. Sci.*, 2013, **8**, 5496–5505.

126 T. V. Vasilache, S. Gutt, I. Sandu, V. Vasilache, G. Gutt, M. Risca and A. V. Sandu, Electrochemical Mechanism of Nickel and Zinc-Nickel Alloy Electrodeposition, *Recent Pat. Corros. Sci.*, 2010, **2**, 1–5.

127 H. Ogihara, M. Fujii and T. Saji, Hydrogen evolution reaction (HER) over electroless-deposited nickel nanospike arrays, *RSC Adv.*, 2014, **4**, 58660–58663.

128 A. Chinnappan, *et al.*, Facile synthesis of electrospun C@NiO/Ni nanofibers as an electrocatalyst for hydrogen evolution reaction, *Int. J. Hydrogen Energy*, 2018, **43**, 15217–15224.

129 S. F. Anis, B. S. Lalia, A. O. Mostafa and R. Hashaikeh, Electrospun nickel–tungsten oxide composite fibers as active electrocatalysts for hydrogen evolution reaction, *J. Mater. Sci.*, 2017, **52**, 7269–7281.

130 Q. Kong, *et al.*, Hydrothermal Synthesis of Nanoporous NiO Rods Self-Supported on Ni Foam as Efficient Electrocatalysts for Hydrogen Evolution Reaction, *JOM*, 2019, **71**, 621–625.

131 P. Sivakumar, *et al.*, Hierarchical NiCo/NiO/$NiCo_2O_4$ composite formation by solvothermal reaction as a potential electrode material for hydrogen evolutions and asymmetric supercapacitors, *Int. J. Energy Res.*, 2021, **45**, 19947–19961.

132 A. Cabrera-García, *et al.*, Bio-inspired Ni dinuclear complexes as heterogeneous catalysts for hydrogen evolution, *Chem. Eng. J.*, 2021, **420**, 130342.

133 A. Gabler, *et al.*, Ultrashort pulse laser-structured nickel surfaces as hydrogen evolution electrodes for alkaline water electrolysis, *Int. J. Hydrogen Energy*, 2017, **42**, 10826–10833.

134 A. Mazzi, *et al.*, Physical vapor deposition of mixed-metal oxides based on Fe, Co and Ni as water oxidation catalysts, *Mater. Sci. Semicond. Process.*, 2016, **42**, 155–158.

135 I. A. Poimenidis, *et al.*, Ni deposition on nickel foam via the use of high-frequency currents for enhanced hydrogen evolution reaction in alkaline media, *J. Phys. Chem. Solids*, 2025, **207**, 112930.

136 A. Lonjon, P. Demont, E. Dantras and C. Lacabanne, Mechanical improvement of P(VDF-TrFE)/nickel nanowires conductive nanocomposites: Influence of particles aspect ratio, *J. Non-Cryst. Solids*, 2012, **358**, 236–240.

137 J. Zhang, W. Xiang, Y. Liu, M. Hu and K. Zhao, Synthesis of High-Aspect-Ratio Nickel Nanowires by Dropping Method, *Nanoscale Res. Lett.*, 2016, **11**, 118.

138 N. Yamasaki, I. R. Korablova and S. F. Korablov, Hydrothermal deposition of nickel on Teflon substrate, *Mater. Lett.*, 2004, **58**, 768–771.

139 I. Poimenidis, E. Skliri, V. Binas, K. Komnitsas and M. Konsolakis, Hydrothermal growth of Co_3O_4 nanoparticles on nickel foam for high-performance pseudocapacitive supercapacitors: Effect of cobalt loading, *Next Mater.*, 2026, **10**, 101449.

140 T. Jiang, *et al.*, Synergistic effects of Ni^{3+}–$Cu^{0/+}$ dual sites for efficient and stable hydrogen production in AEM water electrolysis, *Appl. Catal., B: Environ. Energy*, 2026, **389**, 126597.

141 H. Husin, *et al.*, Efficient hydrogen production by microwave-assisted catalysis for glycerol-water solutions via NiO/zeolite-CaO catalyst, *S. Afr. J. Chem. Eng.*, 2022, **41**, 43–50.

142 X. Hu and J. C. Yu, High-Yield Synthesis of Nickel and Nickel Phosphide Nanowires via Microwave-Assisted Processes, *Chem. Mater.*, 2008, **20**, 6743–6749.

143 M. Mieszkowska and M. Grdeń, Electrochemical deposition of nickel targets from aqueous electrolytes for medical radioisotope production in accelerators: a review, *J. Solid State Electrochem.*, 2021, **25**, 1699–1725.

144 J. Liu, *et al.*, Application of the Electrospinning Technique in Electrochemical Biosensors: An Overview, *Molecules*, 2024, **29**, 2769.

145 K. Ashtari, J. Fasihi, N. Mollania and K. Khajeh, A biotemplated nickel nanostructure: Synthesis, characterization and antibacterial activity, *Mater. Res. Bull.*, 2014, **50**, 348–353.

146 Y. Zhang, *et al.*, Laser Micro/Nano-Structuring Pushes Forward Smart Sensing: Opportunities and Challenges, *Adv. Funct. Mater.*, 2023, **33**, 2211272.

147 A. Cholkar, *et al.*, Advances in laser-based surface texturing for developing antifouling surfaces: A comprehensive review, *Appl. Surf. Sci. Adv.*, 2023, **18**, 100513.

148 A. Klini, A. Manousaki, D. Anglos and C. Fotakis, Growth of ZnO thin films by ultraviolet pulsed-laser ablation: Study of plume dynamics, *J. Appl. Phys.*, 2005, **98**, 123301.

149 N. A. Shepelin, *et al.*, A practical guide to pulsed laser deposition, *Chem. Soc. Rev.*, 2023, **52**, 2294–2321.

150 S. N. Ogugua, O. M. Ntwaeaborwa and H. C. Swart, Latest Development on Pulsed Laser Deposited Thin Films for Advanced Luminescence Applications, *Coatings*, 2020, **10**, 1078.

151 J. Cai, *et al.*, Application of Pulsed Laser Deposition (PLD) Technology in the Preparation of Two-Dimensional (2D) Film Materials, *Materials*, 2025, **18**, 2999.

152 A. K. Eessaa and A. M. El-Shamy, Review on fabrication, characterization, and applications of porous anodic aluminum oxide films with tunable pore sizes for emerging technologies, *Microelectron. Eng.*, 2023, **279**, 112061.

153 I. A. Poimenidis, *et al.*, A novel physical vapor deposition setup applying high-frequency currents: Deposition of Cu thin films, *Vacuum*, 2025, **232**, 113839.

154 S. A. Mahyoub, *et al.*, Physical Vapor Deposition Techniques for CO_2 Electroreduction: A Review, *Small Struct.*, 2025, **6**, 2400501.

155 I. Ledezma-Yanez, *et al.*, Interfacial water reorganization as a pH-dependent descriptor of the hydrogen evolution rate on platinum electrodes, *Nat. Energy*, 2017, **2**, 17031.

156 H. Seenivasan and A. K. Tiwari, Water dissociation on Ni(100) and Ni(111): Effect of surface temperature on reactivity, *J. Chem. Phys.*, 2013, **139**, 174707.

157 A. Mohsenzadeh, K. Bolton and T. Richards, DFT study of the adsorption and dissociation of water on Ni(111), Ni(110) and Ni(100) surfaces, *Surf. Sci.*, 2014, **627**, 1–10.

158 W. Chen, *et al.*, Rationalizing the d-Band Model from Theory to Practice in Catalyst Design, *J. Am. Chem. Soc.*, 2025, **147**, 46729–46744.

159 B. Zhou, *et al.*, Enabling Photon Upconversion and Precise Control of Donor–Acceptor Interaction through Interfacial Energy Transfer, *Adv. Sci.*, 2018, **5**, 1700667.

160 X. Guo, *et al.*, Correlating Boron Existence Morphologies with Electrocatalytic HER Activity in Ni-B Compounds Synthesized via High Pressure and High Temperature, *Catalysts*, 2026, **16**, 65.

161 S. Jo, H. Lee, H. Jang and D. R. Kim, Controlled Integration of Interconnected Pores under Polymeric Surfaces for Low Adhesion and Antiscaling Performance, *ACS Appl. Mater. Interfaces*, 2021, **13**, 13684–13692.

162 L. Mou, T. Han, P. E. S. Smith, E. Sharman and J. Jiang, Machine Learning Descriptors for Data-Driven Catalysis Study, *Adv. Sci.*, 2023, **10**, 2301020.

163 U. Yoon, K. Jeong and S. H. Kim, Advancing electrocatalysis through density functional theory: From reaction mechanisms to machine learning integration, *J. CO_2 Util.*, 2025, **101**, 103192.

164 X. Zhang, *et al.*, Developing Practical Catalysts for High-Current-Density Water Electrolysis, *Adv. Energy Mater.*, 2024, **14**, 2402633.

165 L.-L. Wang, *et al.*, Tailoring Lewis Acidity of Metal Oxides on Nickel to Boost Electrocatalytic Hydrogen Evolution in Neutral Electrolyte, *J. Am. Chem. Soc.*, 2025, **147**, 7555–7563.

166 O. Moyo, *et al.*, Advances in Corrosion-Resistant Metal-Based Oxide Electrocatalysts for Seawater Electrolysis: Focus on Chlorine Mitigation Strategies, *Small*, 2025, **21**, e08973.

167 X. Yang, *et al.*, Bifunctional $Co(PO_3)_2$@Ni_2P/NF interface catalyst for efficient hydrogen production assisted by urea electrooxidation, *J. Electroanal. Chem.*, 2026, **1002**, 119754.

168 C. Liu, *et al.*, Influence of Power Fluctuation on Ni-Based Electrode Degradation and Hydrogen Evolution Reaction Performance in Alkaline Water Splitting: Probing the Effect of Renewable Energy on Water Electrolysis, *Catalysts*, 2024, **14**, 307.

169 J. Wang, *et al.*, Nanoporous Nickel Cathode with an Electrostatic Chlorine-Resistant Surface for Industrial Seawater Electrolysis Hydrogen Production, *Inorg. Chem.*, 2024, **63**, 5773–5778.